

1
2
3
4
5
6
7
8
9
10
11
12
13
14
15
16
17
18
19
20
21
22
23
24
25
26
27
28
29
30
31
32
33
34
35
36
37
38
39
40
41
42
43

Running title *miR-126-3p mediated PVC-matrix interaction*

miR-126-3p promotes matrix-dependent perivascular cell attachment, migration and intercellular interaction

Lena Pitzler^{1,2}, Markus Auler^{1,2}, Kristina Probst^{1,2}, Christian Frie^{1,2}, Vera Bergmeier^{1,2},
Tatjana Holzer^{1,2}, Daniele Belluoccio^{3,4}, Jocelyn Van der Bergen^{3,5}, Julia Etich^{1,2}, Harald
Ehlen^{1,2}, Zhigang Zhou⁶, Wolfgang Bielke, Ernst Pöschl⁶, Mats Paulsson^{2,7,8}, Bent
Brachvogel^{1,2}

¹ Department of Pediatrics and Adolescent Medicine, Experimental Neonatology, Medical
Faculty, University of Cologne, Cologne, Germany

² Center for Biochemistry, Medical Faculty, University of Cologne, Cologne, Germany

³ Murdoch Children's Research Institute, University of Melbourne, Parkville, Victoria,
Australia

⁴ Department of Biochemistry and Molecular Biology, University of Melbourne, Parkville,
Victoria, Australia

⁵ Department of Paediatrics, University of Melbourne, Parkville, Victoria, Australia

⁶ Norwich Medical School, University of East Anglia, Norwich Research Park, Norwich, UK

⁷ Center for Molecular Medicine Cologne (CMMC), University of Cologne, Cologne, Germany

⁸ Cologne Excellence Cluster on Cellular Stress Responses in Aging - Associated Diseases
(CECAD), University of Cologne, Cologne, Germany

° Corresponding author:

Bent Brachvogel

Department of Pediatrics and Adolescent Medicine,

Center for Biochemistry, Medical Faculty,

University of Cologne

Joseph-Stelzmann-Str. 52

D-50931 Cologne

Germany

Tel : +49 221 478 6996,

Fax: +49 221 478 6977,

Email: bent.brachvogel@uni-koeln.de

Key Words

Perivascular cells/miRNA/miR-126-3p/angiogenesis/Spred1/Plk2/Tlr3

Abstract

microRNAs (miRNAs) can regulate the interplay between perivascular cells (PVC) and endothelial cells (EC) during angiogenesis, but the relevant PVC-specific miRNAs are not yet defined. Here, we identified miR-126-3p and miR-146a to be exclusively upregulated in PVC upon interaction with EC, determined their influence on the PVC phenotype and elucidate their molecular mechanisms of action. Specifically the increase of miR-126-3p strongly promoted the motility of PVC on the basement membrane-like composite and stabilized networks of endothelial cells. Subsequent miRNA target analysis showed that miR-126-3p inhibits SPRED1 and PLK2 expression, induces ERK1/2 phosphorylation and stimulates TLR3 expression to modulate cell-cell and cell-matrix contacts of PVC. Gain of expression experiments *in vivo* demonstrated that miR-126-3p stimulates PVC coverage of newly formed vessels and transform immature into mature, less permeable vessels. In conclusion we showed that miR-126-3p regulates matrix-dependent PVC migration and intercellular interaction to modulate vascular integrity.

Introduction

Formation of new blood vessels is normally suppressed in adult tissues. Changes in the local environment upon injury or in tumor formation can induce a neoangiogenic response to provide a blood supply that meets the increased metabolic needs of the injured tissue. Lining endothelial cells (EC) and perivascular cells (PVC) are activated and transform into proliferative, migrating cells to form a new vascular network¹.

PVC can be distinguished according to their abluminal location within the vasculature. Vascular smooth muscle cells are found within arteries, separated by a basement membrane (BM) from the adjacent EC, whereas pericytes are located in the microvasculature enveloped in a BM that they share with EC of small arterioles and capillaries². Such PVC are non-proliferative cells that transform into a migrating and extracellular matrix (ECM)-producing "synthetic" phenotype during neoangiogenesis³.

In recent years it became clear that microRNAs (miRNAs) can play a critical role in vascular cell activation⁴. miRNAs can regulate the expression of multiple genes within cells. Most often a single ~22 nucleotide miRNA binds to complementary sequences within the 3'-untranslated regions (3'-UTR) of target mRNAs and inhibits their translation or promote their degradation⁵. Recent findings indicate that the dysregulation of a single miRNA can impair vascular integrity. *In vivo* downregulation of miR-126 in zebrafish caused vascular leakage and hemorrhage⁶, whereas loss of this miRNA in mice inhibited neointimal lesion formation⁷. Moreover, miR-126 can suppress metastatic angiogenesis⁸ and expression of miR-126 in human was linked to the outcome of chronic heart failure⁹. However, only limited data are available on miRNAs that regulate the interaction of PVC with the extracellular environment and EC.

Previously, we isolated PVC from murine brain meninges and showed that the cells can differentiate into multiple mesenchymal lineages¹⁰, but still maintain their perivascular-like phenotype in culture¹¹. PVC express pericyte-specific markers, stimulate the expression of platelet/endothelial cell adhesion molecule 1 (PECAM1) in human umbilical vein endothelial cells (HUVEC) and promote the deposition of BM proteins. Cocultures of PVC and HUVEC mimic initial steps of angiogenesis and were used in this study to analyze the contribution of miRNAs to PVC interaction with HUVEC. Applying microarray-based miRNA profiling miR-126-3p (corresponding to human miR-126) was identified to be upregulated in cocultured PVC. Transfection of PVC with miR-126-3p mimics strongly promoted integrin β 1-dependent vascular cell contacts on a BM-like composite. Subsequent target analysis revealed that miR-126-3p suppresses the expression of sprouty-related protein with EHV-1 domain 1 (SPRED1), polo-like kinase 2 (PLK2) and insulin receptor 1 substrate (IRS1). Suppression of SPRED1 expression stimulated extracellular signal-regulated kinase 1/2 (ERK1/2) phosphorylation to increase toll-like receptor 3 (TLR3) and chemokine expression and elicited cellular interactions of PVC on matrigel substrate. *In vivo* gain of expression experiments demonstrated that miR-126-3p stimulates neoangiogenesis and vessel stabilization. Hence, miR-126-3p regulates vascular cell recruitment by modulating cell migration on ECM substrates.

Material and Methods

Cell culture

PVC⁹, MC3T3 and b.End5 cells were cultured in DMEM (Gibco) supplemented with 10% FCS, penicillin (100units/ml, Biochrom) and streptomycin (100µg/ml, Biochrom). HUVEC were cultured in Vasculife VEGF-Mv medium (Cell Systems). All experiments were performed at 37°C and 5% CO₂.

For transfection 3×10⁴ cells were resuspended in 550µl of medium and transferred to a 24-well plate. 10nM mimic, 25nM siRNA, 50nM inhibitor or corresponding concentrations of AllStarsNegativeControl in 50µl HiPerFect transfection solution (Qiagen) and DMEM were added. Cells were incubated for 48hours, detached by trypsinization, resuspended in medium additionally supplemented with PDGF (10ng/ml, Biomol) and VEGF (5ng/ml, Biomol) before used in experiments. Downregulation of target genes were validated by qPCR or immunoblotting (see supplemental figure 7).

Cell morphology and migration assays were performed on glass chamber slides (VWR) precoated with 200µl of collagen I (25µg/ml, Gibco), collagen IV (25µg/ml), laminin 511 (20µg/ml, BioLamina), nidogen-1 (25µg/ml), 16µl matrigel (9.1mg/ml, Becton Dickinson) or 16µl of collagen I gel (0.666mg/ml, Gibco) for 1hour at 37°C. 6.5×10³ transfected cells were added and analyzed by microscopy (Nikon TE2000-U, Olympus IX81).

For two-dimensional cocultures transfected PVC were labeled with CFDA-SE and HUVEC were labeled with SNARF-1 according to the suppliers protocol (Invitrogen). Briefly, 1×10⁵ cells were resuspended in 3% FCS/PBS containing 10µM dye and incubated for 15 minutes at 37°C. After washing cells were resuspended in VasculifeVEGF-Mv medium. 8×10³ b.End5 cells were seeded to matrigel-coated wells and after 16 hours 4×10³ PVC were added. 4×10³ PVC and 1.2×10⁴ HUVEC were also added to matrigel-coated wells and cultured for 16hours. The distribution of cells was determined by microscopy.

Three-dimensional cocultures of 5×10⁵ PVC and 2.5×10⁵ HUVEC were established in 400µl of a 2mg/ml rat tail collagen type I gel containing DMEM, 2% FCS, 22.5mM NaHCO₃ and 1mM sodium pyruvate in a 24-well plate. After gelation (37°C, 20 minutes), 400µl EGM-2 medium, 10ng/ml VEGF, 10ng/ml PDGF and 250µg/ml ascorbic acid phosphate were added. Cultures were maintained for five days. Cells were released by digestion with collagenase E (0.4%), collected by centrifugation and washed with PBS. HUVEC were separated from mouse PVC by anti-human PECAM1⁺ Dynabeads (Dyna) selection. Total RNA was isolated from both cell types by RNAeasy Micro kit (Qiagen). Purity of cells was confirmed by immunofluorescence analysis

Proliferation and apoptosis assays

Proliferation was analyzed using the CellTiter 96® AQueous One Solution (Promega) according to the manufacturer's specification. 5×10³ cells were transfected with oligonucleotides in 96-well plates and cultured for two, 24, 48 and 72hours. Substrate was added and production of colored formazan product detected at 492nm using a 96-well plate reader (Sunrise, Tecan). Cell death was determined as described¹². Briefly, PVC were trypsinized 24, 48 and 72hours after transfection, washed, stained with annexin A5 (AnxA5)-Alexa488 and propidium iodide (PI) and analyzed by flow cytometry (FACSCanto II, Becton Dickinson).

RNA isolation and quantification by microarray and quantitative PCR (qPCR)

Total RNA of cells was isolated by phenol-chloroform extraction¹³ and quality was assessed by micro-capillary electrophoresis (2100 Bioanalyzer, Agilent) according to the manufacturer's specifications. For microarray analysis 100ng of purified RNA was labeled and hybridized to mouse or human 8x15K-miRBaseV14 microarrays and to Sureprint-G3 mouse 8x60K whole genome mRNA microarrays using the labeling and hybridization protocol of Agilent. The arrays were scanned (Agilent G2595C scanner), data extracted and processed using the GenespringXII software (Agilent). miRNA or mRNA were selected according to their differential expression, relative expression levels and the statistical significance¹⁴. RNA was also reversely transcribed and used for each prevalidated pri-

1
2
3 miRNA (lifetechnologies) or miRNA-specific SYBR-Green based qPCR assays (Qiagen).
4 The relative expression levels were calculated using the delta-delta C(T) method¹⁵. Data
5 were normalized to the expression of Mapk7 or miR-31.
6
7

8 **Scanning electron microscope analysis**

9 Silicon wafers were precoated with 16µl matrigel for one hour at 37°C. 6.5x10³
10 transfected PVC were added and incubated for four hours. Cells were fixed in 1%
11 glutaraldehyde in PBS for 30minutes at RT and processed for coating with 2nm of platinum.
12 Attachment of cells to the substrate was analyzed by scanning electron microscopy
13 (Leo1530VPGemini, Zeiss).
14

15 **Luciferase reporter assays**

16 Luciferase reporter assays were performed as described¹⁶. Briefly, HEK 293 cells
17 were first transfected with 10nM miR-126-3p mimic or AllStars Negative Control and then
18 cotransfected with 2µg of a psiCHECKTM-2 vector (Promega) which contains the miR-126-3p
19 binding sites. An overview of the oligonucleotides used for the generation of the luciferase
20 reporter constructs is given (supplemental table 1). Luciferase activity was determined using
21 the Dual-Luciferase Reporter Assay System (Promega).
22
23

24 **Immunoblotting**

25 48hours after transfection cells were starved for 45minutes in Vasculife medium
26 without FCS or supplements in the absence or presence of UO126 (10µM)¹⁷ or Wortmannin
27 (2µM, Cell Signaling)¹⁸. Cells were activated with complete Vasculife VEGF-Mv medium.
28 After cell lysis in RIPA buffer equal amounts of protein (20µg) were resolved on 10% SDS-
29 polyacrylamide gels and transferred onto nitrocellulose (Whatman). Immunostainings were
30 performed with primary antibodies detecting pERK1/2, ERK1/2, pAKT, AKT (Cell Signaling),
31 IRS1, SPRED1, GAPDH (Merck Millipore) and PLK2 (Biorbyt) and with the corresponding
32 secondary antibodies labeled with horseradish peroxidase (DAKO). Band intensities were
33 quantified by ImageJ software¹⁹.
34
35

36 ***In vivo* angiogenesis assay**

37 *In vivo* angiogenesis experiments were performed as described²⁰. Briefly, miR-126-
38 3p mimic- or AllStarsNegative control-transfected cells were resuspended in a mixture of
39 matrigel, methocel (Sigma) and fibrinogen (Merck Millipore) containing 500ng/µl VEGF and
40 FGF2 to a final concentration of 500cells/µl. 1µl of thrombin (0.1U/ml, Merck Millipore) was
41 added to 15µl cell suspension, cells were transferred into silicone tubes (Instech) and
42 implanted subcutaneously into the flank of 8 weeks old immunodeficient C.129S6(B6)-
43 Rag2tm1FwaN12 mice. ~16days after implantation 50µl of a FITC-Dextran-70 solution
44 (50µg/ml in H₂O, Sigma) was administered retroorbitally by intravenous injection. Silicone
45 tubes were isolated 25minutes post injection and assessed by microscopy. Matrigel-fibrin
46 plugs were digested in 100µl dispasell (5mg/ml in PBS, Roche) for 45minutes at 37°C,
47 centrifuged for 5minutes at 4°C and 16.000xg and the fluorescence was determined by
48 fluorescence spectroscopy (Infinite M1000, Tecan).
49
50

51 **Statistical analysis**

52 The statistical analyses were performed with Student's t-test using the unpaired two-
53 tails method. p-values<0.05(*) were considered to be statistically significant, p-
54 values<0.005(**)-highly significant. Standard deviations are indicated.
55
56
57
58
59
60

Results

miR-126-3p is upregulated in PVC upon interaction with HUVEC

To identify miRNAs that are upregulated in PVC upon interaction with EC three-dimensional cocultures of PVC and HUVEC were established. In monocultures of HUVEC or PVC (supplemental Figure 1) only few tubes were formed after five days in three-dimensional collagen I gels, whereas the number and length of tubes was markedly increased in cocultures (Figure 1A). Immunodetection of PECAM1 demonstrated that the tubes contain a significant amount of HUVEC (Figure 1B). Total RNA was isolated from PVC or HUVEC monocultures and cocultures of immunomagnetically separated PVC with HUVEC. The purity of the isolated cell population was confirmed by immunofluorescence analysis (supplemental Figure 1). RNA was subjected to microarray analysis and the transcriptome was screened for differentially and significantly expressed miRNAs (Figure 1C). Several miRNAs were significantly downregulated in cocultured PVC. Of note is that only two of 690 analyzed miRNAs were highly abundant in cocultured but absent in monocultured PVC, namely miR-126-3p and miR-146a (Figure 1D, F). Both miRNAs were also expressed in HUVEC but not regulated during coculture (Figure 1E). Therefore, the two miRNAs were specifically upregulated upon PVC-HUVEC interaction only in PVC. Their regulation was then validated by qPCR analysis. A strong upregulation for miR-126-3p and a less pronounced upregulation for miR-146a was detected in this assay (Figure 1G). Characterization of the pri-miRNA expression by qPCR also indicated that the increase in miR-126-3p was accompanied by an upregulation of its pri-miRNA in cocultured PVC (Figure 1H). Hence, we hypothesized that miRNA-126-3p and miR-146a are needed to promote PVC interaction with EC to maintain vascular integrity.

miR-126-3p promotes migration and interaction of PVC on matrigel

PVC and EC are connected via a BM and miR-126-3p and miR-146a may modulate the binding of PVC to BM-proteins, which was analyzed by cell-matrix interaction experiments. miR-126-3p or miR-146a levels were increased in PVC using synthetic RNAs that mimic mature endogenous miRNAs (mimics) or nonspecific control oligonucleotides. The complex BM-like matrigel was coated on glass chamber slides, transfected PVC were added 48 hours post transfection and cell morphology was determined. Interestingly, miR-126-3p mimic-transfected PVC, but not miR-146a mimic- or control-transfected cells, formed cell aggregates connected by filamentous structures (Figure 1I). Therefore, the analysis was focused on the miR-126-3p in PVC. Quantification of aggregate-associated filaments 16 hours after seeding on matrigel showed that cumulative length of filamentous links between aggregates were fivefold increased in miR-126-3p mimic-transfected PVC compared to control. In contrast, transfection of an anti-miR-126-3p oligonucleotide caused a decrease in length of aggregate-associated links (supplemental Figure 2A). Non-perivascular MC3T3 cells failed to form links after increasing miR-126-3p levels by transfection when compared to PVC in time lapse microscopy (supplemental Figure 2B). The results indicated that the cell-cell interaction on BM-like matrigel is mainly promoted by increased levels of miR-126-3p.

miR-126-3p upregulation in PVC may also promote intercellular interaction with EC, which we analyzed in coculture experiments. Control- or miR-126-3p mimic-transfected, fluorescently labeled PVC were added to preformed networks of mouse brain derived endothelial cells (b.End5 cells) on matrigel. The PVC were rapidly incorporated into endothelial networks 7 hours after seeding (Figure 2A). Networks containing control-transfected PVC partially disassembled after 14 hours, whereas networks containing miR-126-3p mimic-transfected PVC were stabilized. In addition, fluorescently labeled control- or miR-126-3p mimic-transfected PVC (green) and HUVEC (red) were added to matrigel-coated chamber slides and cultured for 16 hours. Network-like structures formed on the matrigel substrate in cocultures of HUVEC and control-transfected PVC (Figure 2B). These were mainly composed of HUVEC (red). In contrast, a large number of PVC was detected in networks of cocultures with miR-126-3p mimic-transfected PVC. Hence, miR-126-3p supported the interaction of PVC and EC on BM-like composites.

1
2
3
4 Next we analyzed the phenotype of PVC on single BM-components. PVC adapted a
5 spindle-like morphology on glass and on laminin 511, collagen I, collagen IV and nidogen-1
6 (Figure 3A). No differences in morphology or cell numbers were observed between control-
7 and miR-126-3p mimic-transfected cells and aggregates and filamentous structures were not
8 formed. Hence, miR-126-3p modulated the PVC phenotype on complex BM-like substrates
9 but not on single BM-components. Time lapse microscopy revealed that miR-126-3p mimic-
10 transfected PVC formed multipolar protrusions on matrigel and within four hours cell
11 aggregates appeared, whereas control-transfected PVC still maintained a round morphology
12 (Figure 3B). After seven hours aggregates formed long directional protrusions to contact
13 more distant cells and assembled into larger cell clusters. Control-transfected cells formed
14 small protrusions 12 hours after plating but were unable to form large aggregates and long
15 protrusions. Quantification of cell migration showed that trajectory and the intervals to form
16 cell-cell contacts were reduced in mimic-transfected cells compared to control, while the
17 covered distance and the average speed per cell was unchanged (Figure 3C). 90% of the
18 miR-126-3p mimic-transfected PVC were involved in cell-cell interaction and most cells
19 remained in aggregates throughout the incubation time. In contrast, only 60% of the control-
20 transfected PVC formed aggregates with about half of these remaining in aggregates
21 (supplemental video). Scanning electron microscopy illustrated the effect of miR-126-3p
22 on the morphology of PVC (Figure 3D). After cultivation for four hours on matrigel, miR-126-3p
23 mimic-transfected PVC formed long directional protrusions through cell-cell contacts to
24 assemble thin and long filamentous links on the matrigel surface, while control-transfected
25 cells showed few multipolar protrusions. Therefore, increased abundance of miR-126-3p
26 promoted intercellular contacts of PVC specifically on matrigel.

27
28 Cell-matrix and cell-cell interactions are mainly mediated by β 1-integrin cell surface
29 receptors. siRNA-mediated knock down approach was used to demonstrate that β 1-integrin
30 contributes to the miR-126-3p mimic induced phenotype in PVC. Control- or miR-126-3p
31 mimic-transfected PVC were transfected with siRNAs directed against β 1-integrin and 48
32 hours later added to matrigel coated chamber slides. After four hours network formation was
33 studied (Figure 3E). Cells transfected with siRNA against β 1-integrin lost the ability to form
34 aggregates and network-associated links but showed a spindle-like morphology. This
35 resembled the phenotype of control- or miR-126-3p mimic-transfected PVC cultured on glass
36 or on single BM substrates (Figure 3A). No differences between control- and miR-126-3p
37 mimic-transfected PVC were detected. The results pointed to a role of β 1-integrin-mediated
38 formation of aggregates and intercellular connections.

41 miR-126-3p targets *Spred1*, *Plk2*, and *Irs1* and activates the ERK signaling pathway in 42 PVC

43 Target scan database analysis revealed that 20 conserved target genes are
44 predicted for the miR-126-3p, but only a few may represent true targets of the miRNA. We
45 hypothesized that target genes need to be expressed in the vasculature to modulate the
46 activity of major signaling pathways and induce aggregate and protrusion formation of PVC.
47 Therefore, gene expression atlas analysis (www.genepaint.org) and web-based literature
48 search was used to exclude targets that were not described to be expressed in the
49 vasculature and were not known to be involved in signaling pathway modulation. Among the
50 20 target genes SPRED1 and phosphatidylinositol 3-kinase regulatory subunit polypeptide 2
51 (PIK3R2) could regulate the activation of AKT and ERK1/2 signaling pathways in EC⁶ and
52 IRS1 was described to be a target of miR-126-3p in smooth muscle cells⁷. In addition, the
53 signaling proteins regulator of G-protein signaling 3 (RGS3) and PLK2 were expressed in the
54 developing vasculature of the mouse embryo^{21,22}. Hence, we focused our analysis on
55 SPRED1, PIK3R2, IRS1, RGS3 and PLK2. First, we studied the interaction of miR-126-3p
56 with its binding sequences in the 3'-UTR of selected target genes using luciferase assays¹⁶.
57 The luciferase activity was significantly reduced in miR-126-3p mimic-transfected HEK293
58 cells that contain the miR-126-3p binding sequence of *Spred1*, *Plk2* or *Irs1* in the 3'-UTR of
59 the luciferase reporter gene (Figure 4A). The inhibitory effect was abolished by two point
60 mutations within the binding sequences of *Spred1*, *Plk2* or *Irs1*, demonstrating the specificity

1
2
3
4 of the miR-126-3p interaction. The luciferase activity was not decreased in cells containing
5 the miR-126-3p 3'-UTR binding sequences of *Pik3r2* and *Rgs3*. Interestingly, the luciferase
6 activity was reduced for the binding sequence of the human *PIK3R2* gene, pointing to
7 species-specific differences in target gene recognition. In conclusion, miR-126-3p interacted
8 with the 3'-UTR of mouse *Spred1*, *Irs1* and *Plk2*.

9
10 Next, their expression was studied in an existing mRNA microarray dataset (E.
11 Pöschl, unpublished results) of the three-dimensional coculture system and in immunoblot
12 analysis. The selected target genes were expressed in three-dimensional monocultures of
13 PVC. The mRNA expression of *Plk2* and *Irs1* was reduced in PVC upon coculture with
14 HUVEC (Figure 4B) and in immunoblot analysis a significant twofold reduction was found for
15 all proteins in miR-126-3p mimic-transfected PVC compared to control (Figure 4C). To study
16 the role of each target gene in PVC migration and interaction PVC were transfected with
17 siRNAs directed against *Spred1*, *Plk2* or *Irs1* and added to matrigel-coated chamber slides.
18 16 hours later network formation was compared to control- or miR-126-3p mimic-transfected
19 PVC. *siSpred1*- and *siPlk2*- transfected PVC formed network-like structures as seen for miR-
20 126-3p mimic-transfected PVC, whereas control- and *siIrs1*-transfected PVC formed only
21 few multipolar protrusions (Figure 4D). The cumulative tube length was fivefold increased in
22 miR-126-3p mimic-transfected PVC and fourfold in PVC transfected with *siSpred1* and
23 *siPlk2* compared to control- or *siIrs1*-transfected PVC. In contrast, aggregate and network-
24 associated link formation was inhibited when overexpressing SPRED1 in miR-126-3p mimic-
25 transfected PVC (supplemental Figure 3). Taken together, SPRED1 and IRS1 are regulatory
26 targets of miR-126-3p and PLK2 was identified as a novel target of miR-126-3p in PVC.
27 Inhibition of SPRED1 and PLK2 expression could mimic the effect of miR-126-3p in PVC on
28 matrigel and the phenotype of miR-126-3p mimic-transfected PVC could be rescued by
29 SPRED1 overexpression.

30
31 miR-126 can repress SPRED1 expression to stimulate the activation of the ERK1/2
32 and AKT signaling pathways in human EC⁶. We asked whether the pathways were also
33 targeted in murine PVC. Cells were transfected with control or miR-126-3p mimic
34 oligonucleotides or with siRNAs directed against *Spred1*, *Plk2* or *Irs1*, cultured on plastic and
35 stimulated with serum. ERK1/2 phosphorylation was determined 15 minutes later (Figure
36 5A). ERK1/2 phosphorylation was significantly increased in miR-126-3p mimic- and
37 *siSpred1*-transfected PVC compared to control, whereas phosphorylation was not affected in
38 *siPlk2*- or *siIrs1*-transfected cells. This indicated that increased miR-126-3p levels inhibit
39 *Spred1* expression to modulate ERK1/2 phosphorylation in PVC. The phosphorylation status
40 of ERK1/2 of control- or miR-126-3p mimic-transfected PVC was assessed in (Figure 5B) 5,
41 15 and 30 minutes after stimulation with complete VasculLife VEGF-Mv medium. In addition,
42 AKT phosphorylation was analyzed. The amounts of pERK1/2 were significantly increased in
43 miR-126-3p mimic-transfected PVC, whereas pAKT was not significantly increased
44 compared to control. Hence, miR-126-3p mainly stimulated ERK1/2 phosphorylation in PVC.

45
46 To demonstrate that cell-cell and cell-matrix interactions were induced by ERK1/2 but
47 not by AKT signaling pathway activation we cultured control- and miR-126-3p mimic-
48 transfected PVC for 16 hours on matrigel in the presence of 10 μ M U0126 inhibitor to
49 suppress the phosphorylation of ERK1/2 or 2 μ M Wortmannin to inhibit AKT phosphorylation.
50 The addition of U0126 blocks aggregate-associated link formation in miR-126-3p mimic-
51 transfected PVC, but not the addition of Wortmannin (Figure 5C). The inhibition of ERK1/2 or
52 AKT phosphorylation was confirmed by immunoblot analysis indicating that both inhibitors
53 acted specifically on their individual kinases (Figure 5D). Therefore, only the inhibition of
54 ERK1/2 phosphorylation blocked aggregate-associated link formation in miR-126-3p mimic-
55 transfected PVC.

56 57 58 **miR-126-3p stimulates chemokine expression in PVC**

59
60 The miR-126-3p-mediated activation of the ERK1/2 signaling pathway could induce
downstream changes to stimulate cell-matrix and cell-cell contacts. These changes were
studied by global transcriptome analysis using a 60k whole genome array of control- and
miR-126-3p mimic-transfected cells after four hours culture on matrigel, when multipolar

1
2
3 protrusions and cell aggregates start to form in miR-126-3p mimic but not in control-
4 transfected PVC. To determine the influence of miR-126-3p on genes involved in cell-matrix
5 interaction we initially studied the expression of vascular basement membrane proteins and
6 integrin receptors. Collagens, fibronectin, perlecan, laminins and nidogens and the
7 corresponding integrin receptors were not differentially expressed in miR-126-3p mimic-
8 transfected PVC compared to control (supplemental Figure 4A). We then focused on
9 significantly upregulated and annotated genes in miR-126-3p mimic-transfected PVC (Figure
10 6A). 47 upregulated genes were imported into the String 9.1 database and functional
11 partnerships between the imported entities were determined. 38 genes were clustered and
12 seven were linked to cytokine-cytokine receptor interaction (supplemental Figure 4B).
13 Among those chemokine (C-C motif) ligand 5 (*Ccl5*) was reported to promote endothelial cell
14 migration, spreading and neo-vessel formation²³. Chemokine production can be regulated by
15 mitogen activated kinases via the Toll-like receptor 3 (*Tlr3*)^{24,25} and this was an upregulated
16 cell surface receptor in miR-126-3p transfected PVC. The ECM can interact with Toll-like
17 receptors²⁶ and TLR3 can mediate endothelial cell migration and vascular sprouting²⁷.
18
19 Hence, CCL5 and TLR3 may promote PVC migration and interaction upon miR-126-3p
20 mimic transfection in PVC on matrigel. To study their function we performed siRNA-mediated
21 knock down studies and transfected control- or miR-126-3p mimic-transfected PVC with
22 siRNAs directed against *Ccl5* or *Tlr3*. PVC were added to matrigel and 16 hours later
23 formation of network-like structures was analyzed (Figure 6B). PVC transfected with
24 *siCcl5* and miR-126-3p mimic formed network-like structures, whereas PVC transfected with
25 *siTlr3* and miR-126-3p mimic showed only few multipolar protrusions. The cumulative tube
26 length was fourfold decreased compared to *siCcl5* or control-transfected PVC with elevated
27 levels of the miR-126-3p. Therefore, miR-126-3p induced, presumably through increased
28 ERK1/2 phosphorylation, TLR3 expression in PVC on matrigel to stimulate PVC migration and
29 intercellular interaction, whereas induced CCL5 expression was not needed for cell-matrix
30 and cell-cell contacts.

31 32 33 **miR-126-3p modulates PVC-dependent angiogenesis *in vivo***

34 To analyze the role of miR-126-3p *in vivo* we used a directed *in vivo* angiogenesis
35 assay²⁰. Control- or mimic-transfected PVC were transferred to a silicone tube in a matrigel-
36 fibrin matrix enriched in VEGF and FGF2 and tubes were implanted subcutaneously under
37 the dorsal skin of immunodeficient mice. ~16 days after implantation, matrigel-fibrin
38 plugs were isolated and vascular invasion was assessed by microscopy. Matrigel-fibrin plugs
39 containing control-transfected PVC were invaded by few vessels and small blood lacunae
40 were formed (Figure 7A). In contrast the anterior and central area of the plugs containing
41 miR-126-3p mimic-transfected cells were highly vascularized. Newly formed vessels
42 deeply infiltrated the matrix and blood lacunae were detected. Vascularization and permeability of
43 the newly formed vessels was assessed by intravenously injection of a FITC-dextran
44 tracer (70kDa) prior to isolation of the tubes. This tracer can diffuse into the extracellular space
45 of immature vessels but is retained in mature, less permeable vessels²⁸. A diffuse staining of
46 the matrigel-fibrin matrix was seen for plugs containing control-transfected cells 30
47 minutes after injection, whereas a strong vessel associated staining was observed for
48 plugs containing miR-126-3p mimic-transfected cells (Figure 7B). These FITC-dextran positive
49 vessels originate from the anterior end to form a vascular tree branching into the central area
50 of the plug. The matrigel-fibrin matrix and blood lacunae were hardly stained. The
51 accumulation of the FITC-dextran conjugate in plugs was also analyzed by fluorescence
52 spectroscopy. Plugs were digested with dispase, centrifuged and the fluorescence of the
53 supernatant was determined at 510nm (Figure 7C). The fluorescence signal was significantly
54 increased for plugs containing miR-126-3p mimic-transfected cells compared to control. The
55 results show that miR-126-3p mimic-transfected PVC induced a strong angiogenic response
56 *in vivo*. The lack of FITC-dextran leakage into the perivascular space demonstrated that the
57 newly formed vasculature was stabilized by perivascular cells.
58
59
60

Discussion

Blood vessel formation and stabilization depends on the control of interactions between perivascular and endothelial cells. Our analysis identified murine miR-126-3p (corresponding to human miR-126) to be selectively upregulated in PVC upon interaction with EC to promote BM-dependent migration and mutual interactions.

Originally, miR-126 was described to increase the migration of human EC in scratch assays and reduced levels affected the stability of tubes formed on matrigel substrate⁶. The present study shows for the first time that increased levels of miR-126-3p in murine PVC stimulate formation of network-like assemblies on matrigel, a composite substrate resembling a BM. In contrast, individual components of the vascular BM, e. g. laminin 511, collagen IV and nidogen 1 failed to promote network-formation. Knock down of β 1-integrin in miR-126-3p mimic-transfected PVC resulted in the loss of aggregate formation and cultures on collagen I gels failed to form any networks (supplemental Figure 5). The results indicate that miR-126-3p promotes integrin-mediated synergistic interaction of PVC with more than one BM component and, most likely, with vascular BM.

miR-126 was described to induce SMC proliferation and apoptosis⁷. We could not observe changes in PVC proliferation or survival (supplemental Figure 6), which could be due to the use of different culture systems in the two studies. Here, PVC were transfected with miR-126-3p mimic to determine the direct effects of the miRNA upregulation on the cellular phenotype, whereas in the earlier study EC were transfected with inhibitors of miR-126-3p and indirect effects on SMC survival were analyzed. This suggests that secondary signals transmitted from EC in response to changes in miR-126-3p expression modulate survival and proliferation of cocultured PVC rather than direct effects of miR-126-3p on PVC.

We focused on the consequences of increased miR-126-3p expression in PVC since miR-126-3p is strongly upregulated in PVC upon interaction with EC. Nevertheless, inhibition of miR-126-3p caused a significant reduction in network formation, demonstrating that limited levels of miR-126-3p were present in PVC monocultures and modulated the PVC response to matrigel. In PVC specifically the miR-126 3'-strand modulates the interaction with the ECM environment. The effect is mediated by activating the ERK1/2 signaling pathway as we could demonstrate that miR-126-3p suppresses SPRED1 protein expression in PVC to stimulate ERK1/2 phosphorylation leading to network-like structure formation. Moreover, we could block matrix-dependent intercellular interactions in miR-126-3p mimic-transfected PVC by ERK1/2 pathway inhibition or SPRED1 overexpression. This is in line with previous reports showing that miR-126-3p can inhibit SPRED1 expression to increase the activation of the ERK1/2 pathway in human EC⁶. SPRED1, a member of the sprouty-related protein with EHV-1 domain (SPRED) family of proteins, can translocate to the membrane to down-regulate Ras-GTP levels and inhibit the ERK1/2 signaling pathway²⁹. Knock down of miR-126 in zebrafish stimulated SPRED1 expression and enhanced ERK1/2 signal pathway activation and resulted in the loss of vascular integrity and hemorrhage during embryonic development⁶. This was mainly attributed to altered ERK1/2 signal pathway activation in endothelial cells. Our study now points to an additional role of the miR-126-3p-SPRED1-ERK1/2 axis in PVC and in cell-matrix interactions. We also showed that *Irs1* is downregulated by miR-126-3p in PVC upon coculture with EC. A previous study demonstrated that miR-126-3p represses IRS1 protein expression in cocultured SMC⁷, but the relevance for the cellular phenotype is less clear. PVC attachment and cellular interactions are not affected upon *Irs1* knock down and PLK2 as a novel target for the miR-126-3p in PVC seems to be of greater significance. PLK2 belongs to the polo-like family of serine/threonine kinases, which can modulate dendritic spine remodeling in neurons^{30,31}. Interestingly, the siRNA-mediated knock down of PLK2 protein, which is expressed in the vasculature and is a direct target of miR-126-3p, also promotes PVC protrusion formation on matrigel. The molecular link between reduced PLK2 activity and the stimulation of PVC-EC interactions on BM-like composites is not yet known. The siRNA studies indicated that ERK and AKT signaling pathways are not targeted by PLK2, but recent results linked PLK2 to the TLR signaling response³².

1
2
3
4 In contrast, SPRED1-dependent suppression of ERK1/2 signaling pathway seems to
5 be an essential molecular link. The inhibitor studies showed that an impaired ERK1/2
6 phosphorylation blocks network-like tube formation of PVC and we identified that
7 downstream chemokine-receptor targets that are upregulated upon culture of miR-126-3p
8 mimic-transfected PVC on a matrigel substrate. Several of these cytokines are associated
9 with the toll-like-receptor pathway and only recently it was shown that miR-126-3p can
10 control the expression of Toll-like receptor genes in dendritic cells³³. Interestingly, *Tlr3*
11 mRNA expression was also significantly increased upon culturing of miR-126-3p transfected
12 PVC on matrigel substrate. *Tlr3* mRNA expression can be stimulated by ERK1/2 signaling²⁴
13 and TLR3 signaling can augment the production of chemokines²⁵. Although Toll-like receptor
14 signaling is mainly related to the innate immune response and recognition of dsRNA³⁴ a
15 recent report showed that Toll-like receptors can also recognize ECM molecules²⁶ and
16 promote endothelial cell migration and vascular sprouting²⁷. We showed that in PVC miR-
17 126-3p can reduce SPRED1 protein levels to induce ERK1/2 phosphorylation, increase *Tlr3*
18 mRNA expression and modulate PVC-matrix interaction and network-like structure
19 formation. Hence, miR-126-3p-induced ERK1/2 phosphorylation and *Tlr3* upregulation fulfill
20 important functions during vascular homeostasis.

21 These findings are relevant in the context of new vessel formation in normal
22 and pathological angiogenesis, where deposition of basement membranes is critical for EC-
23 PVC interactions and stabilization of the maturing vessels. The upregulation of miR-126-3p
24 in PVC upon coculture with EC, the increased cell-matrix and cell-cell contacts upon miR-
25 126-3p transfection as well as the proangiogenic and vessel-stabilizing effects *in vitro* and *in*
26 *in vivo* suggest that miR-126-3p promotes the maturation of newly formed vessels. The effects
27 are mainly mediated by the inhibition of PLK2 and SPRED1. PLK2 downregulation by miR-
28 126-3p overexpression induces phenotypic changes in PVC irrespective of ERK activation,
29 whereas SPRED1 downregulation by miR-126-3p overexpression induces changes via
30 stimulation of the ERK signaling pathway. The latter is in line with a previous published link
31 between SPRED1 and ERK phosphorylation in endothelial cells³⁵. As a consequence
32 increased miR-126-3p levels stimulate matrix-dependent intercellular interaction of PVC to
33 promote coverage of newly formed vessel and transform immature into mature, less
34 permeable vessels. In contrast, decreased miR-126-3p levels may loosen basement
35 membrane-dependent intercellular connections and support detachment of PVC and EC
36 from preexisting vessels to allow new blood vessel formation. Hence, miR-126-3p modulates
37 basement membrane-dependent PVC migration and cell-cell contacts in the neovasculature.
38 We therefore propose that miR-126-3p is a novel regulator of PVC-mediated vessel stability
39 during neoangiogenesis and in pathological scenarios like tumor angiogenesis.
40
41
42
43
44

45 **Acknowledgements**

46 DFG (SFB829-B04, DFG 2304/5-3, 2304/7-1, 2304/9-1), Köln Fortune - University of
47 Cologne (136/2013, 120/2014). We thank Katrin Blumbach for her support in live cell
48 imaging and Manuel Koch and Manuel Keller for providing collagen IV and nidogen-1.
49
50
51
52
53
54
55
56
57
58
59
60

References

1. Etich J, Bergmeier V, Frie C, et al. PECAM1(+)/Sca1(+)/CD38(+) Vascular Cells Transform into Myofibroblast-Like Cells in Skin Wound Repair. *PLoS ONE*. 2010;8:e53262.
2. Sims DE. The pericyte--a review. *Tissue Cell*. 1986;18:153-174.
3. Owens GK, Kumar MS, Wamhoff BR. Molecular regulation of vascular smooth muscle cell differentiation in development and disease. *Physiol Rev*. 2004;84:767-801.
4. Kane NM, Thrasher AJ, Angelini GD, et al. Concise review: MicroRNAs as modulators of stem cells and angiogenesis. *Stem Cells*. 2014;32:1059-1066.
5. Gordeladze JO, Djouad F, Brondello JM, et al. Concerted stimuli regulating osteo-chondral differentiation from stem cells: phenotype acquisition regulated by microRNAs. *Acta Pharmacol Sin*. 2009;30:1369-1384.
6. Fish JE, Santoro MM, Morton SU, et al. miR-126 regulates angiogenic signaling and vascular integrity. *Dev Cell*. 2008;15:272-284.
7. Zhou J, Li JY, Nguyen P, et al. Regulation of Vascular Smooth Muscle Cell Turnover by Endothelial Cell-secreted MicroRNA-126: Role of Shear Stress. *Circ Res*. 2013.
8. Png KJ, Halberg N, Yoshida M, et al. A microRNA regulon that mediates endothelial recruitment and metastasis by cancer cells. *Nature*. 2011;481:190-194.
9. Qiang L, Hong L, Ningfu W, et al. Expression of miR-126 and miR-508-5p in endothelial progenitor cells is associated with the prognosis of chronic heart failure patients. *Int J Cardiol*. 2013.
10. Brachvogel B, Moch H, Pausch F, et al. Perivascular cells expressing annexin A5 define a novel mesenchymal stem cell-like population with the capacity to differentiate into multiple mesenchymal lineages. *Development*. 2005;132:2657-2668.
11. Brachvogel B, Pausch F, Farlie P, et al. Isolated Anxa5(+)/Sca-1(+) perivascular cells from mouse meningeal vasculature retain their perivascular phenotype in vitro and in vivo. *Exp Cell Res*. 2007;313:2730-2743.
12. Rosenbaum S, Kreft S, Etich J, et al. Identification of novel binding partners (annexins) for the cell death signal phosphatidylserine and definition of their recognition motif. *J Biol Chem*. 2011;286:5708-5716.
13. Chomczynski P, Sacchi N. Single-step method of RNA isolation by acid guanidinium thiocyanate-phenol-chloroform extraction. *Anal Biochem*. 1987;162:156-159.
14. Smyth GK. Linear models and empirical bayes methods for assessing differential expression in microarray experiments. *Stat Appl Genet Mol Biol*. 3, Article3. 2004:1-26.
15. Pfaffl MW. A new mathematical model for relative quantification in real-time RT-PCR. *Nucleic Acids Res*. 2001;29:e45.
16. Etich J, Holzer T, Pitzler L, et al. MiR-26a modulates extracellular matrix homeostasis in cartilage. *Matrix Biol*. 2015;43:27-34.
17. Chow S, Patel H, Hedley DW. Measurement of MAP kinase activation by flow cytometry using phospho-specific antibodies to MEK and ERK: potential for pharmacodynamic monitoring of signal transduction inhibitors. *Cytometry*. 2001;46:72-78.
18. Arcaro A, Wymann MP. Wortmannin is a potent phosphatidylinositol 3-kinase inhibitor: the role of phosphatidylinositol 3,4,5-trisphosphate in neutrophil responses. *Biochem J*. 1993;296 (Pt 2):297-301.
19. Rasband W. ImageJ. U. S. National Institutes of Health, Bethesda, Maryland, USA. 1997-2011.
20. Guedez L, Rivera AM, Salloum R, et al. Quantitative assessment of angiogenic responses by the directed in vivo angiogenesis assay. *Am J Pathol*. 2003;162:1431-1439.
21. Couplier F, Le Crom S, Maro GS, et al. Novel features of boundary cap cells revealed by the analysis of newly identified molecular markers. *Glia*. 2009;57:1450-1457.
22. Visel A, Thaller C, Eichele G. GenePaint.org: an atlas of gene expression patterns in the mouse embryo. *Nucleic Acids Res*. 2004;32:D552-556.

- 1
2
3
4
5
6
7
8
9
10
11
12
13
14
15
16
17
18
19
20
21
22
23
24
25
26
27
28
29
30
31
32
33
34
35
36
37
38
39
40
41
42
43
44
45
46
47
48
49
50
51
52
53
54
55
56
57
58
59
60
23. Suffee N, Hlawaty H, Meddahi-Pelle A, et al. RANTES/CCL5-induced pro-angiogenic effects depend on CCR1, CCR5 and glycosaminoglycans. *Angiogenesis*. 2012;15:727-744.
 24. Peroval MY, Boyd AC, Young JR, et al. A critical role for MAPK signalling pathways in the transcriptional regulation of toll like receptors. *PLoS One*. 2013;8:e51243.
 25. Mitchell D, Olive C. Regulation of Toll-like receptor-induced chemokine production in murine dendritic cells by mitogen-activated protein kinases. *Mol Immunol*. 2010;47:2065-2073.
 26. Schaefer L, Babelova A, Kiss E, et al. The matrix component biglycan is proinflammatory and signals through Toll-like receptors 4 and 2 in macrophages. *J Clin Invest*. 2005;115:2223-2233.
 27. Thuringer D, Jego G, Wettstein G, et al. Extracellular HSP27 mediates angiogenesis through Toll-like receptor 3. *FASEB J*. 2013;27:4169-4183.
 28. Machado MJ, Mitchell CA. Temporal changes in microvessel leakiness during wound healing discriminated by in vivo fluorescence recovery after photobleaching. *The Journal of physiology*. 2011;589:4681-4696.
 29. Stowe IB, Mercado EL, Stowe TR, et al. A shared molecular mechanism underlies the human rasopathies Legius syndrome and Neurofibromatosis-1. *Genes Dev*. 2012;26:1421-1426.
 30. Lee KJ, Lee Y, Rozeboom A, et al. Requirement for Plk2 in orchestrated ras and rapsignaling, homeostatic structural plasticity, and memory. *Neuron*. 2013;69:957-973.
 31. Pak DT, Sheng M. Targeted protein degradation and synapse remodeling by an inducible protein kinase. *Science*. 2003;302:1368-1373.
 32. Chevrier N, Mertins P, Artyomov MN, et al. Systematic discovery of TLR signaling components delineates viral-sensing circuits. *Cell*. 2011;147:853-867.
 33. Agudo J, Ruzo A, Tung N, et al. The miR-126-VEGFR2 axis controls the innate response to pathogen-associated nucleic acids. *Nat Immunol*. 2014;15:54-62.
 34. Alexopoulou L, Holt AC, Medzhitov R, et al. Recognition of double-stranded RNA and activation of NF-kappaB by Toll-like receptor 3. *Nature*. 2001;413:732-738.
 35. Meng S, Cao JT, Zhang B, et al. Downregulation of microRNA-126 in endothelial progenitor cells from diabetes patients, impairs their functional properties, via target gene Spred-1. *J Mol Cell Cardiol*. 2012;53:64-72.

Figures

Figure 1

Identification of miRNAs regulated in PVC in three-dimensional cocultures with HUVEC

Microscopic analysis of HUVEC monocultures and HUVEC/PVC cocultures. (A) Formation of tube-like structures is strongly promoted in three-dimensional cocultures. (B) Detection of PECAM1 by immunofluorescence analysis. (C-F) The miRNA transcriptome between mono- (Mo) and cocultured (Co) PVC or HUVEC was compared using miRNA-array (Agilent) analyses based on the Sanger miRBase release 14. (C) Intensity plot includes all miRNAs detected in PVC. (D) Plot of regulated miRNAs expressed in PVC (fold change ≥ 2 , p-value ≥ 0.01) that show a signal intensity above background noise. The non-regulated miR-31 was used for normalization. (E) Intensity plot showing all miRNAs detected in HUVEC. The expression of miR-126 and miR-146a is highlighted (green). (F) Calculated fold changes for miR-126-3p, miR-146a and miR-31 are listed. (G) miRNA and (H) pri-miR-126-3p expression was validated by quantitative PCR (qPCR). Microarray and qPCR analyses were performed in two or three independent biological experiments, respectively. (I) Cell cluster and protrusion formation of miR-126-3p or miR-146a mimic-transfected PVC on matrigel-coated surfaces 16 hours post plating compared to control-transfected PVC.

Figure 2

Characterization of PVC-EC interaction on matrigel

(A) Time lapse images of fluorescently labeled control- or miR-126-3p mimic-transfected PVC (green) added to preformed networks of b.End5 cells. The cumulative tube length of three independent experiments was determined at 14h hours (graph). (B) Coculture of fluorescently labeled control- (green, left) or miR-126-3p mimic-transfected PVC (green, right) and HUVEC (red) on matrigel 16 hours post plating. The HUVEC⁺ or PVC⁺ pixel/area of three independent experiments were determined (graph). Representative images are shown.

Figure 3

Analysis of cell morphology and migration of control- or miR-126-3p mimic-transfected PVC

(A) Morphology of transfected PVC on uncoated (glass) or ECM protein-coated surfaces 15 hours after adding the cells to the various substrates. (B) Representative time lapse images of cell attachment and migration on matrigel. Individual cells are numbered. (C) Cell migration parameters like distance, trajectory, speed and time until cell-cell contact were determined for three independent experiments. (D) Scanning electron microscopy illustrates the morphology of control- and miR-126-3p mimic-transfected PVC four hours after plating on matrigel. (E) Aggregate and protrusion formation of control- and miR-126-3p mimic-transfected PVC after siRNA-mediated knock down of $\beta 1$ -integrin on matrigel-coated surface 4 hours post plating.

Figure 4

Identification of miR-126-3p-dependent target genes and signaling pathways in PVC

(A) Interaction of miR-126-3p with the intact or mutated (mut) putative binding site in the 3'-UTR of the indicated target genes. Fold changes of Renilla to Firefly luciferase activity in miR-126-3p mimic-transfected cells compared to control-transfected cells are presented. (B) Heatmap to illustrate the expression of miR-126-3p target genes in mono- (Mo) or cocultured (Co) PVC analyzed by mRNA microarray. (C) Extracts of control- and miR-126-3p mimic-transfected PVC analyzed for the presence of SPRED1, PLK2 and IRS1 by immunoblotting. GAPDH detection was used as loading control. Fold change of SPRED1, PLK2 or IRS1 to GAPDH ratio in miR-126-3p mimic-transfected cells compared to control- (graph). (D) Cell cluster and protrusion formation of control-, miR-126-3p mimic- and siRNA-transfected PVC on matrigel-coated surface 16 hours post plating. The individual target

genes of each siRNA are indicated. The cumulative tube length of three independent experiments was quantified (graph).

Figure 5

Silencing of target genes in PVC on matrigel-coated surfaces and consequences for ERK1/2 and AKT signaling

(A) Immunoblot analysis of ERK1/2 signaling pathway activation 15 minutes after serum stimulation in control-, miR-126-3p mimic- or siRNA-transfected PVC on plastic. The molecular weight of ERK1 and ERK2 is given. The fold change in phosphorylation normalized to total ERK1/2 in miR-126-3p mimic-transfected cells compared to control for five independent experiments is shown (graph). (B) Representative immunoblot showing phosphorylated (p) ERK1/2, total ERK1/2 (upper panel), pAKT and total AKT (lower panel) in control- and miR-126-3p mimic-transfected PVC after serum stimulation. The fold change in phosphorylation in miR-126-3p mimic-transfected cells compared to control-transfected cells normalized to total ERK1/2 or AKT was determined. The results of four or more independent experiments 15 minutes after stimulation are summarized (graph). (C) Aggregate and protrusion formation of control- and miR-126-3p mimic-transfected PVC in the presence of 10 μ M U0126 or 2 μ M Wortmannin on matrigel-coated surface 16 hours post plating. (D) Immunoblot analysis of ERK1/2 and AKT phosphorylation in treated PVC 15 minutes after serum stimulation.

Figure 6

Determination of transcriptome changes in miR-126-3p mimic-transfected PVC on matrigel-coated surfaces

The mRNA transcriptome of control- and miR-126-3p mimic-transfected PVC was compared four hours post plating on matrigel. Four independent experiments were analyzed using whole genome mRNA-arrays (Agilent). (A) Intensity expression plot of differentially expressed genes. The fold change (FC) is shown. (B) Aggregate and network formation of control-, miR-126-3p mimic- and siRNA-transfected PVC on a matrigel-coated surface 16 hours post plating. The individual target genes of each siRNA are indicated. The cumulative tube length of three independent experiments was determined (graph).

Figure 7

Characterization of proangiogenic effects by miR-126-3p mimic-transfected PVC *in vivo*

(A) Microscopic assessment of neoangiogenesis in subcutaneously implanted silicone tubes (angioreactors) filled with control- or miR-126-3p mimic-transfected cells. Angioreactors were isolated from immunodeficient mice 14-17 days after implantation. Three representative angioreactors for control- and mimic-transfected PVC are shown. (B) FITC-Dextran-70 solution was injected intravenously 30 minutes prior isolation of the angioreactors to stain newly formed vessels. Fluorescence microscopy analysis was used to determine the distribution and permeability of newly formed vessels. All images were simultaneously adjusted in brightness, contrast and color. (C) Quantification of FITC-Dextran-70 in the supernatant of dispase-digested angioreactors by fluorescence spectrometry.

Figure 1

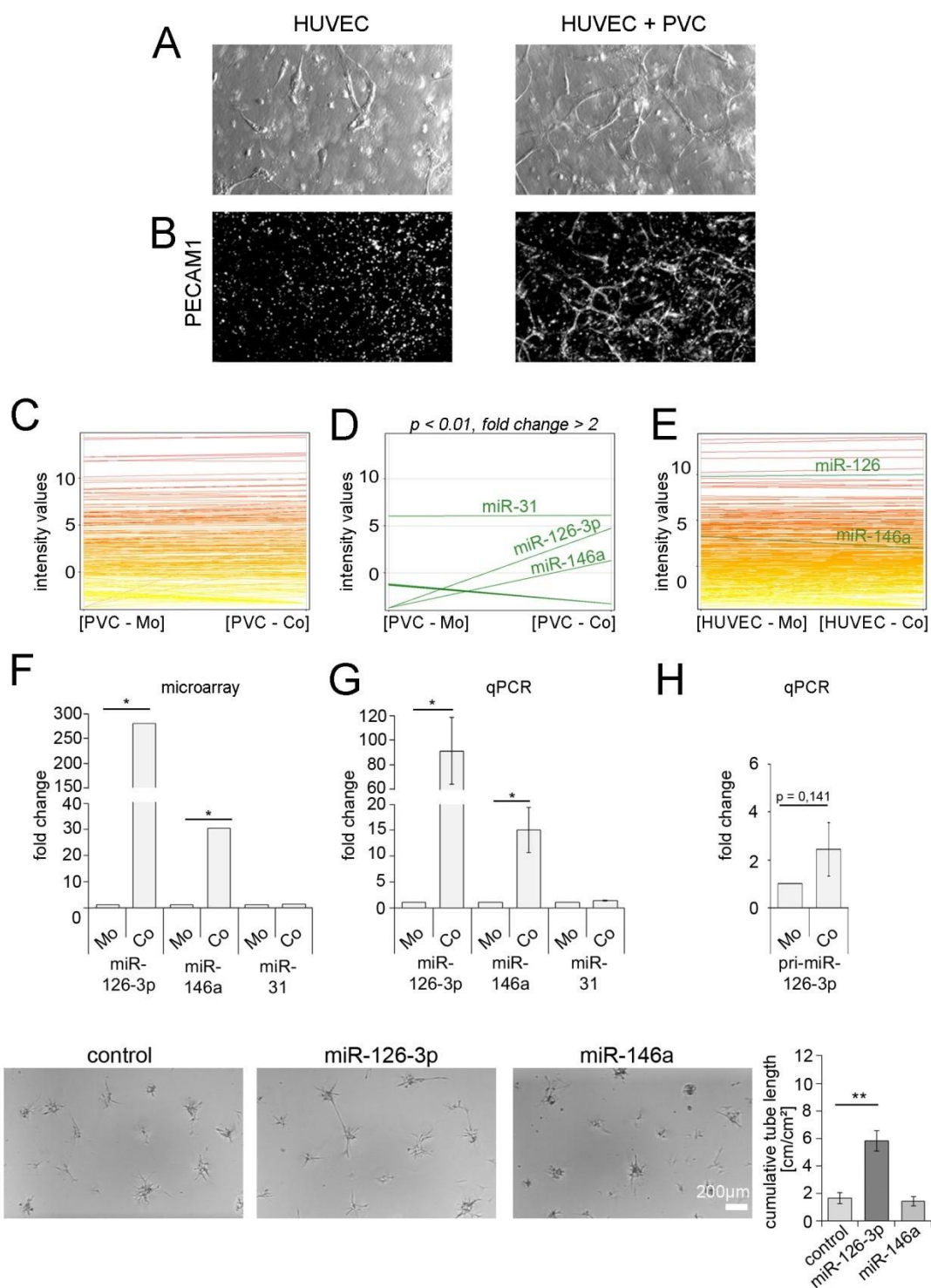


Figure 2

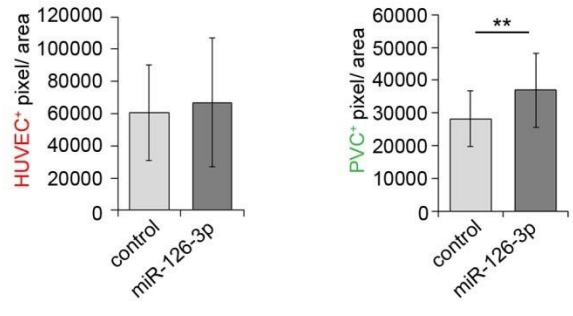
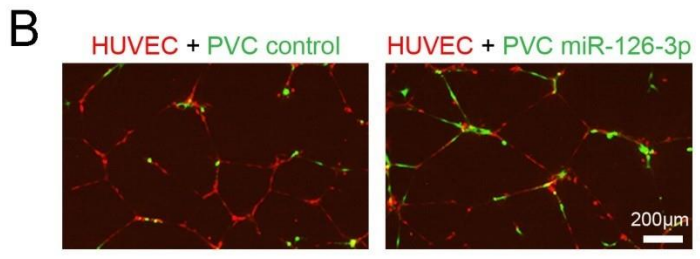
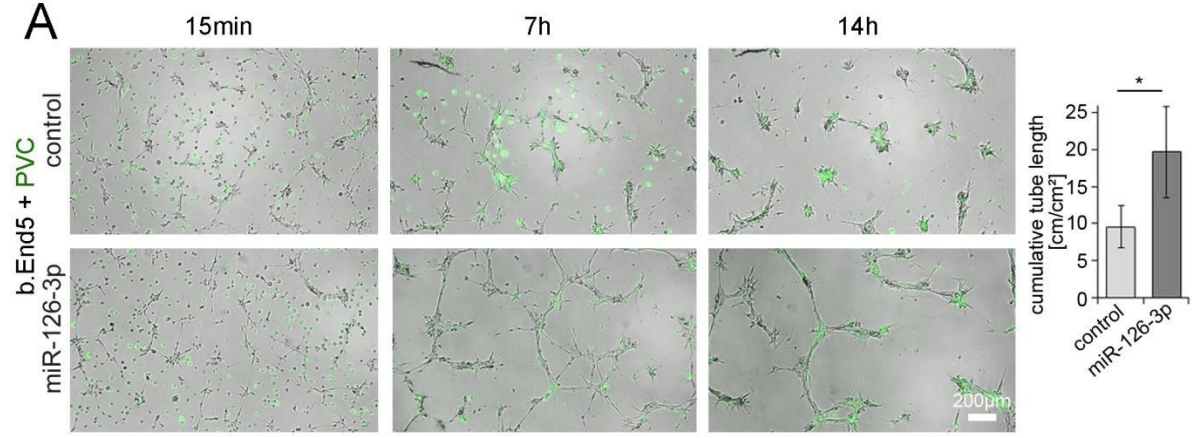


Figure 3

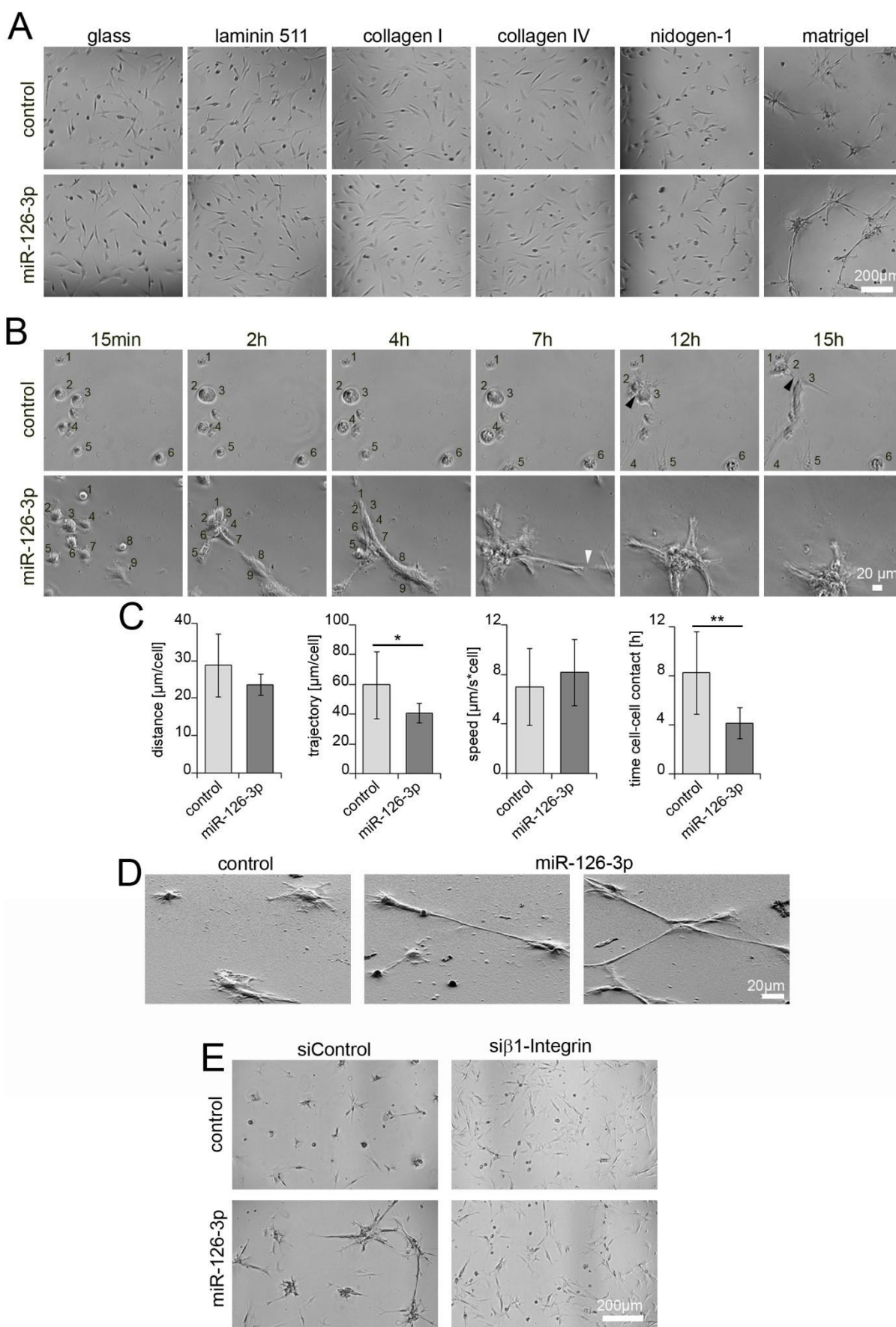


Figure 4

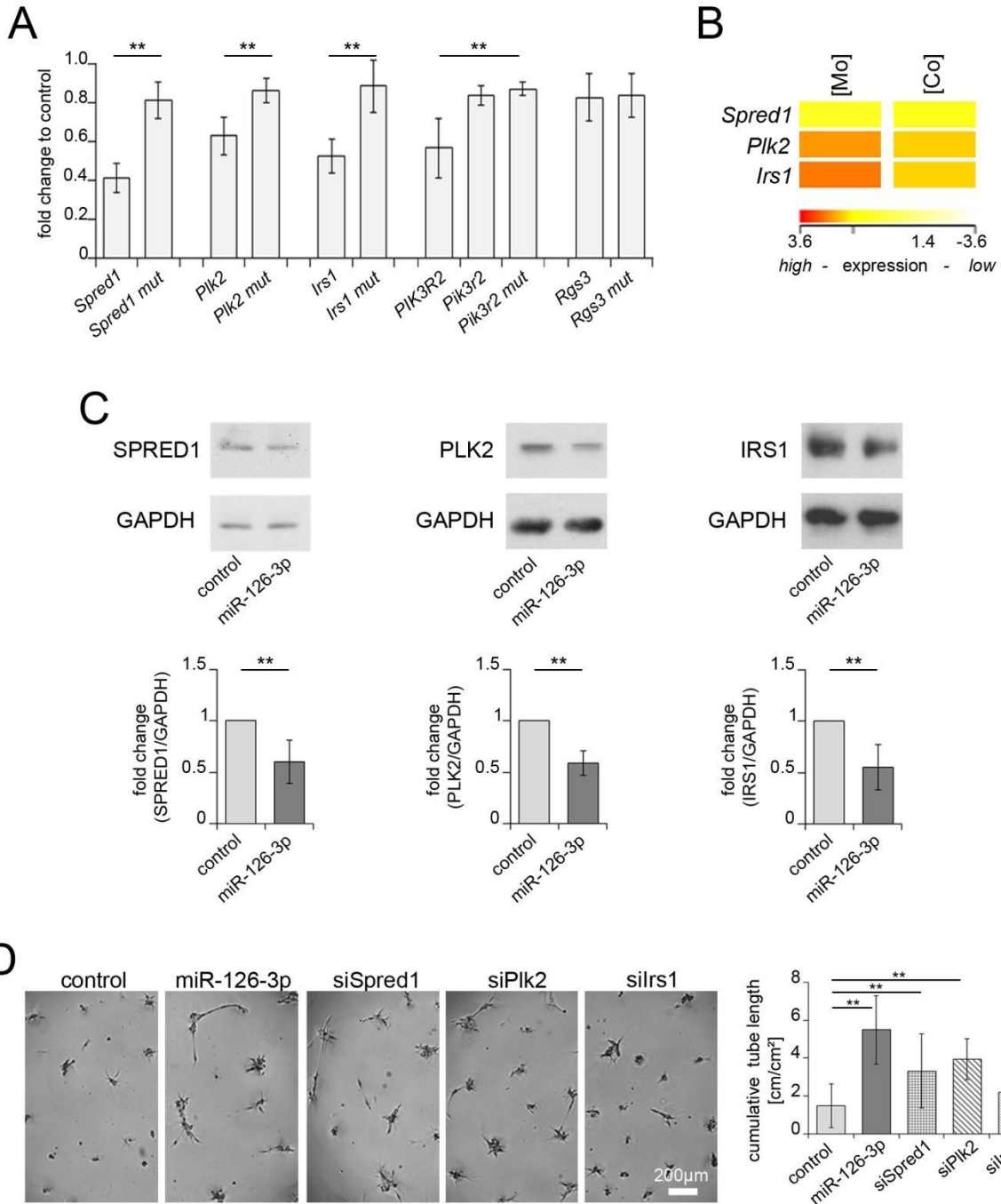


Figure 5

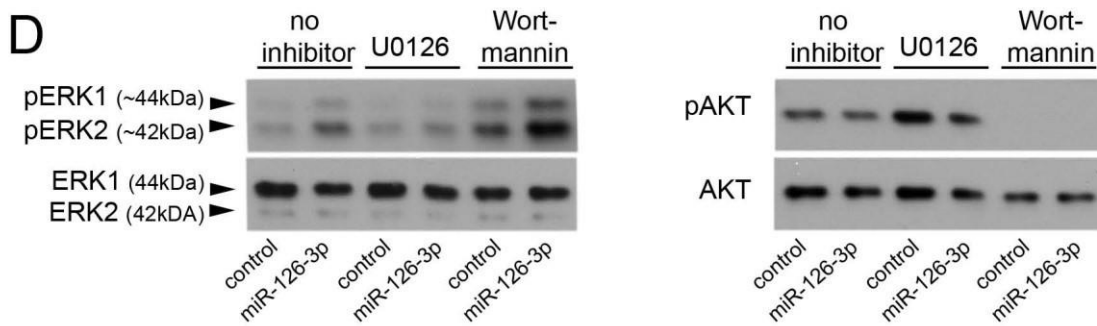
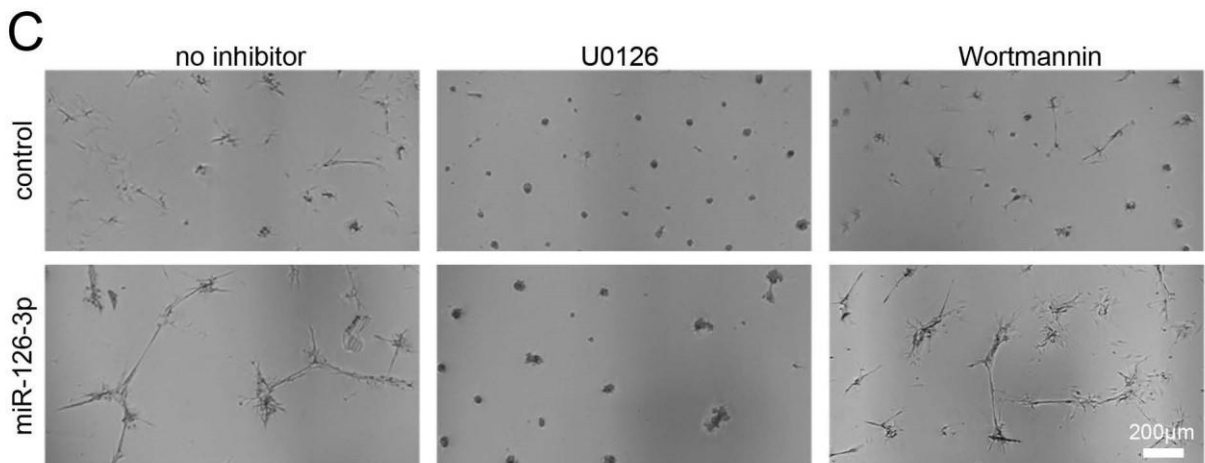
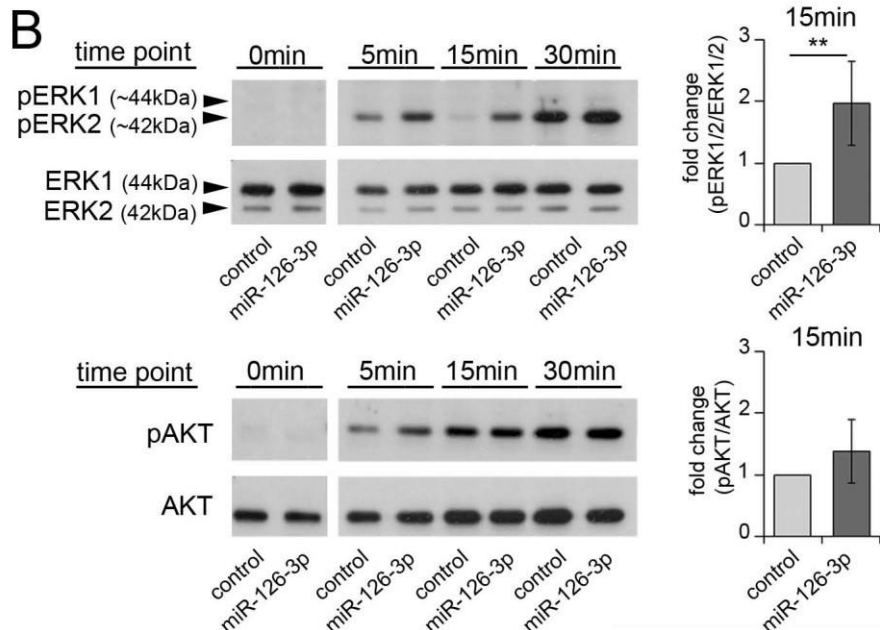
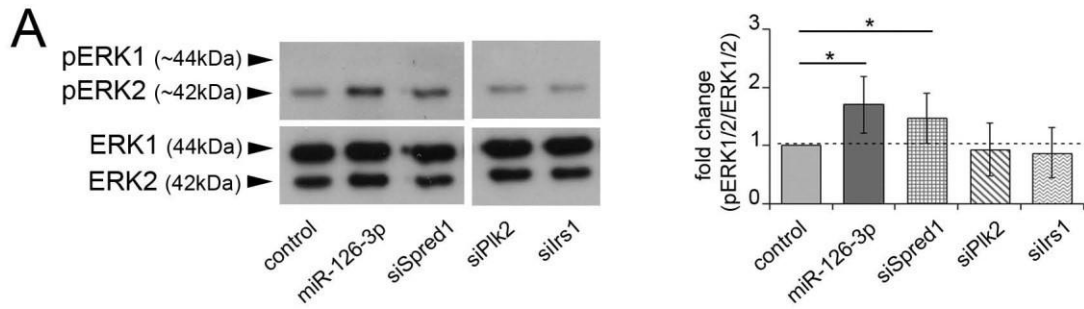


Figure 6

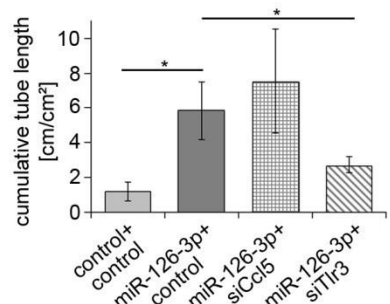
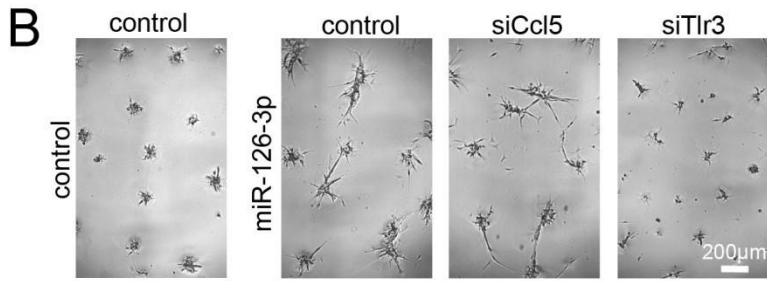
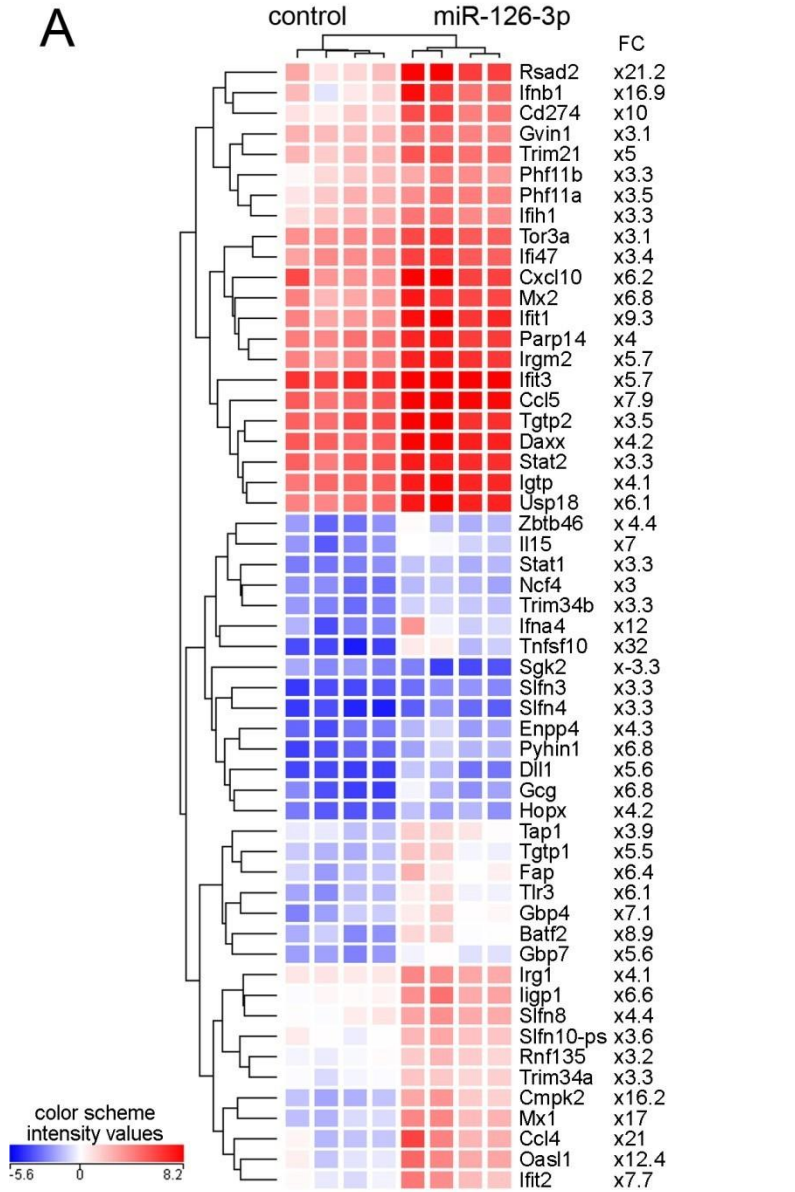
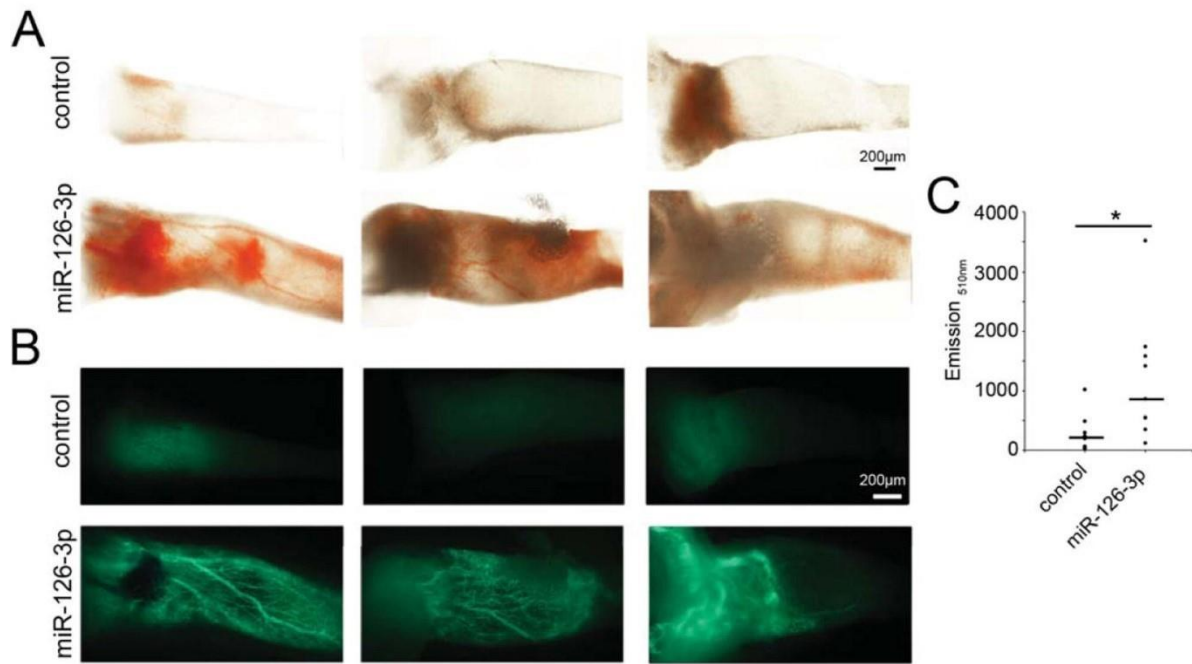
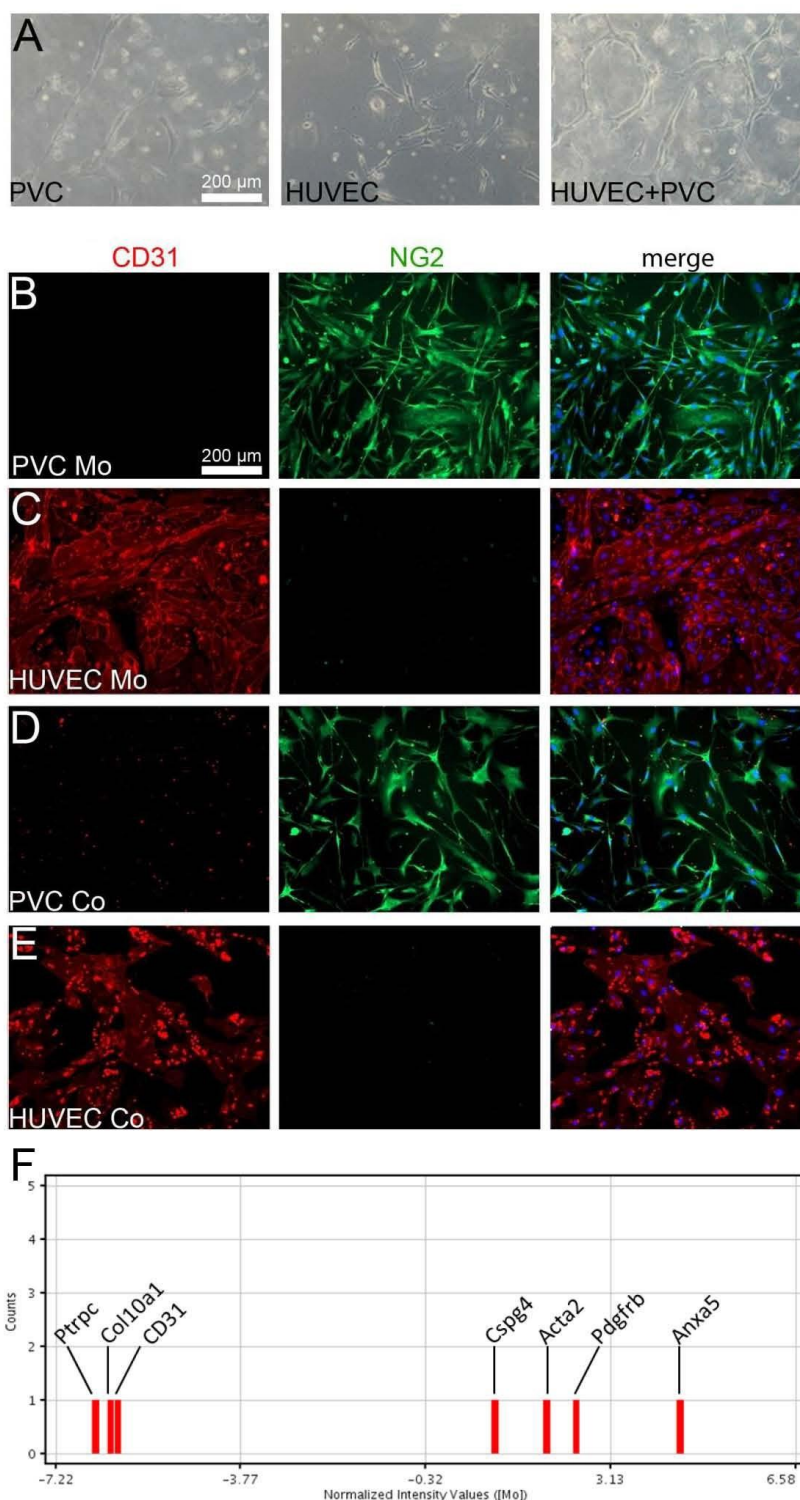


Figure 7



1
2
3
4
5
6
7
8
9
10
11
12
13
14
15
16
17
18
19
20
21
22
23
24
25
26
27
28
29
30
31
32
33
34
35
36
37
38
39
40
41
42
43
44
45
46
47
48
49
50
51
52
53
54
55
56
57
58
59
60



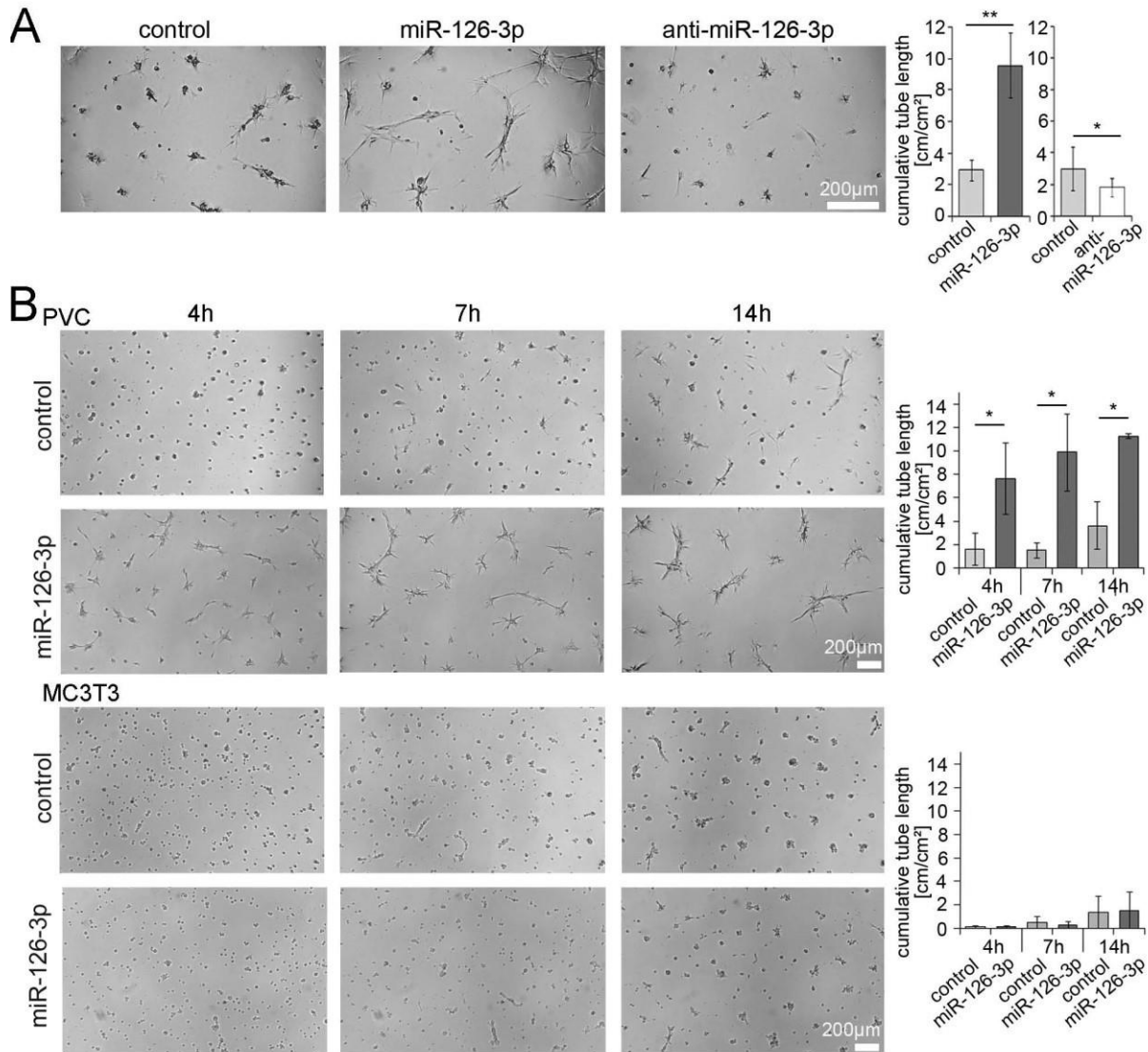
Supplemental Figure 1

Characterization of the purity of separated PVC and HUVEC from three-dimensional cocultures

(A) Microscopic analysis of PVC and HUVEC monocultures and HUVEC/PVC cocultures.

Formation of tube-like structures is strongly promoted in three dimensional cocultures. (B-E) Detection of EC- (PECAM1 (CD31)) and PVC-specific (NG2) marker gene expression by immunofluorescence in PVC and HUVEC monocultures (B, C, Mo) and in immunomagnetically separated PVC and HUVEC from cocultures (D, E, Co) 24 hours after separation and cultivation on plastic. (F) Microarray analysis of selected marker genes in

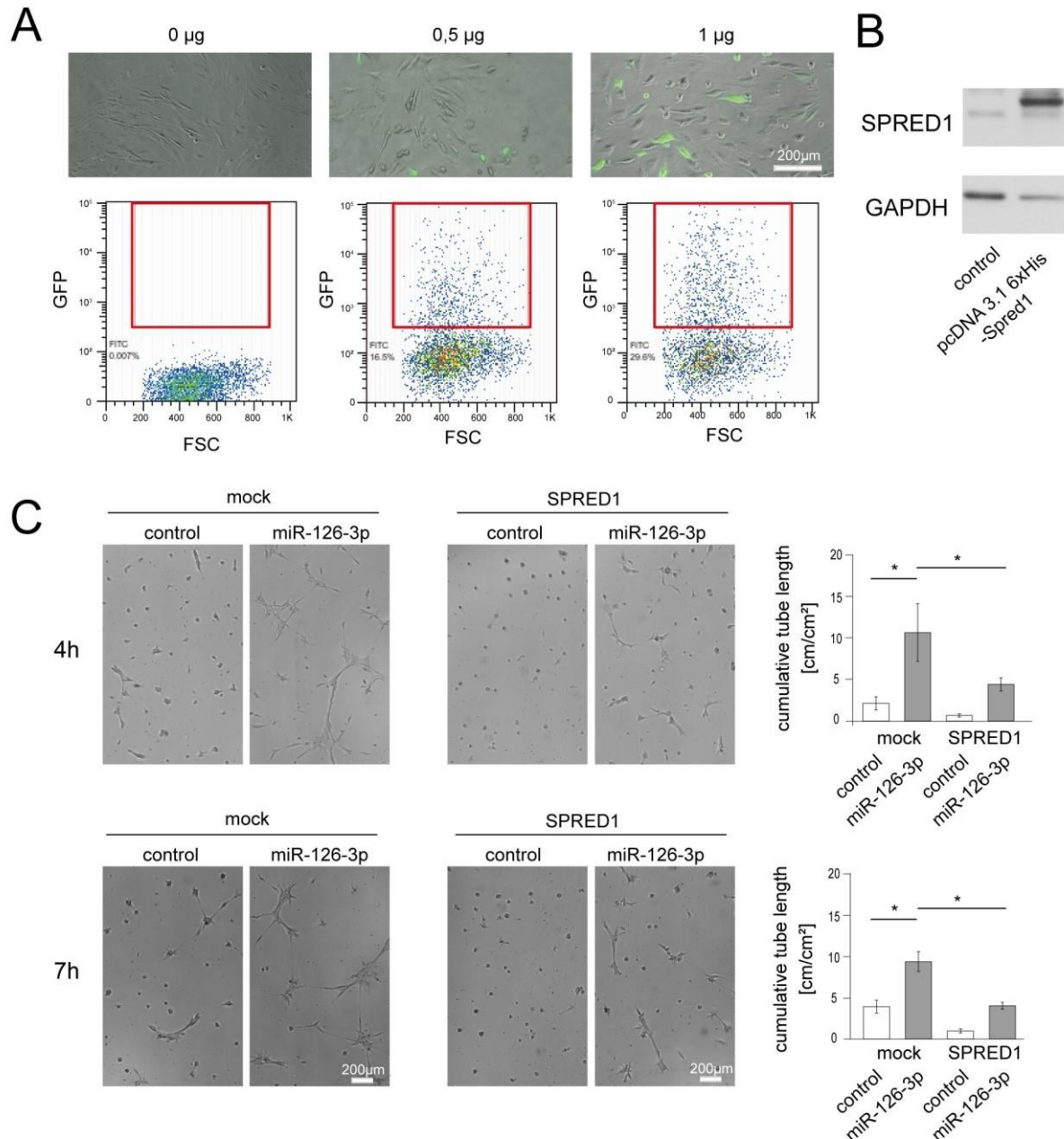
1
2
3 purified PVC. Normalized intensity values of selected genes in whole genome transcriptome
4 analysis are displayed for cocultured cells. Counts correspond to the number of detected
5 probes for a specific gene. Transcripts specific for hypertrophic chondrocytes (Col10a1) or
6 leukocytes (Ptrpc (CD45)) define the background signal of expression. Genes coding for
7 endothelial cell markers Pecam1 (CD31) and perivascular cell markers (Cspg4 (Ng2), Acta2
8 (a-Sma), Pdgfrb and Anxa5) are shown. The analysis confirms that PVC and HUVEC can
9 successfully be separated from cocultures and used in downstream experiments.
10
11
12
13
14
15
16
17
18
19
20
21
22
23
24
25
26
27
28
29
30
31
32
33
34
35
36
37
38
39
40
41
42
43
44
45
46
47
48
49
50
51
52
53
54
55
56
57
58
59
60



Supplemental Figure 2

Phenotypic analysis of control- or mimic-transfected cells

(A) Cell cluster and protrusion formation of control, miR-126-3p mimic or inhibitor-transfected PVC (anti-miR-126-3p) on matrigel-coated surfaces 16 hours post plating compared to control-transfected PVC. (B) Time lapse images of control- or miR-126-3p mimic-transfected PVC and MC3T3 cells. The cumulative tube length was determined in three independent experiments (graph). Representative images are shown.



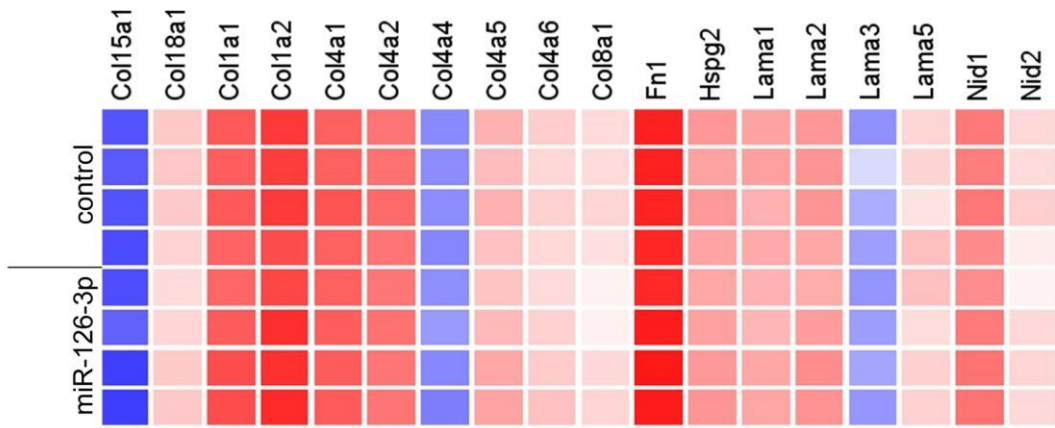
Supplemental Figure 3

Expression of recombinant SPRED1 inhibits aggregate and protrusion formation in miR-126-3p mimic-transfected PVC on matrigel-coated surfaces

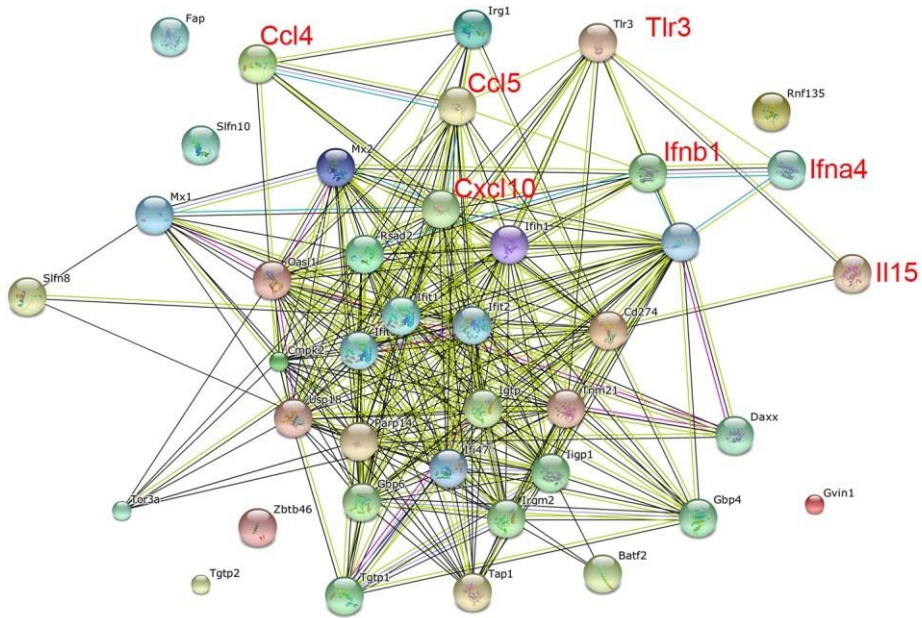
(A) Microscopy and flow cytometry analysis of GFP expression in pmaxGFP-transfected PVC. (B) Representative immunoblot showing the overexpression of SPRED1 in pcDNA 3.1 6xHis-Spred1-transfected PVC. (C) Time lapse images of mock or pcDNA 3.1 6xHis-Spred1 transfected PVC (SPRED1) containing control or miR-126-3p mimics. The cumulative tube length was determined for three independent experiments (graph). Representative images four and seven hours post plating are shown.

1
2
3
4
5
6
7
8
9
10
11
12
13
14
15
16
17
18
19
20
21
22
23
24
25
26
27
28
29
30
31
32
33
34
35
36
37
38
39
40
41
42
43
44
45
46
47
48
49
50
51
52
53
54
55
56
57
58
59
60

A



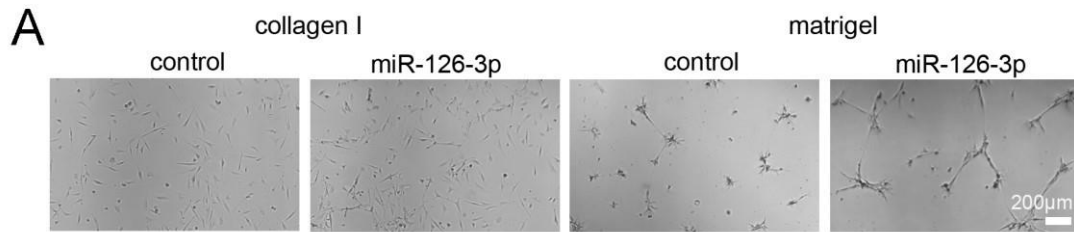
B



Supplemental Figure 4

Transcriptome analysis of control and miR-126-3p mimic-transfected PVC

The mRNA transcriptome of control- and miR-126-3p mimic-transfected PVC was compared four hours post plating on matrigel using whole genome mRNA arrays (Agilent). (A) Intensity expression plot of vascular basement membrane entities. The values for four individual experiments are shown. (B) String database analysis plot of expressed and regulated mRNA (fold change ≥ 2 , p-value ≤ 0.01).



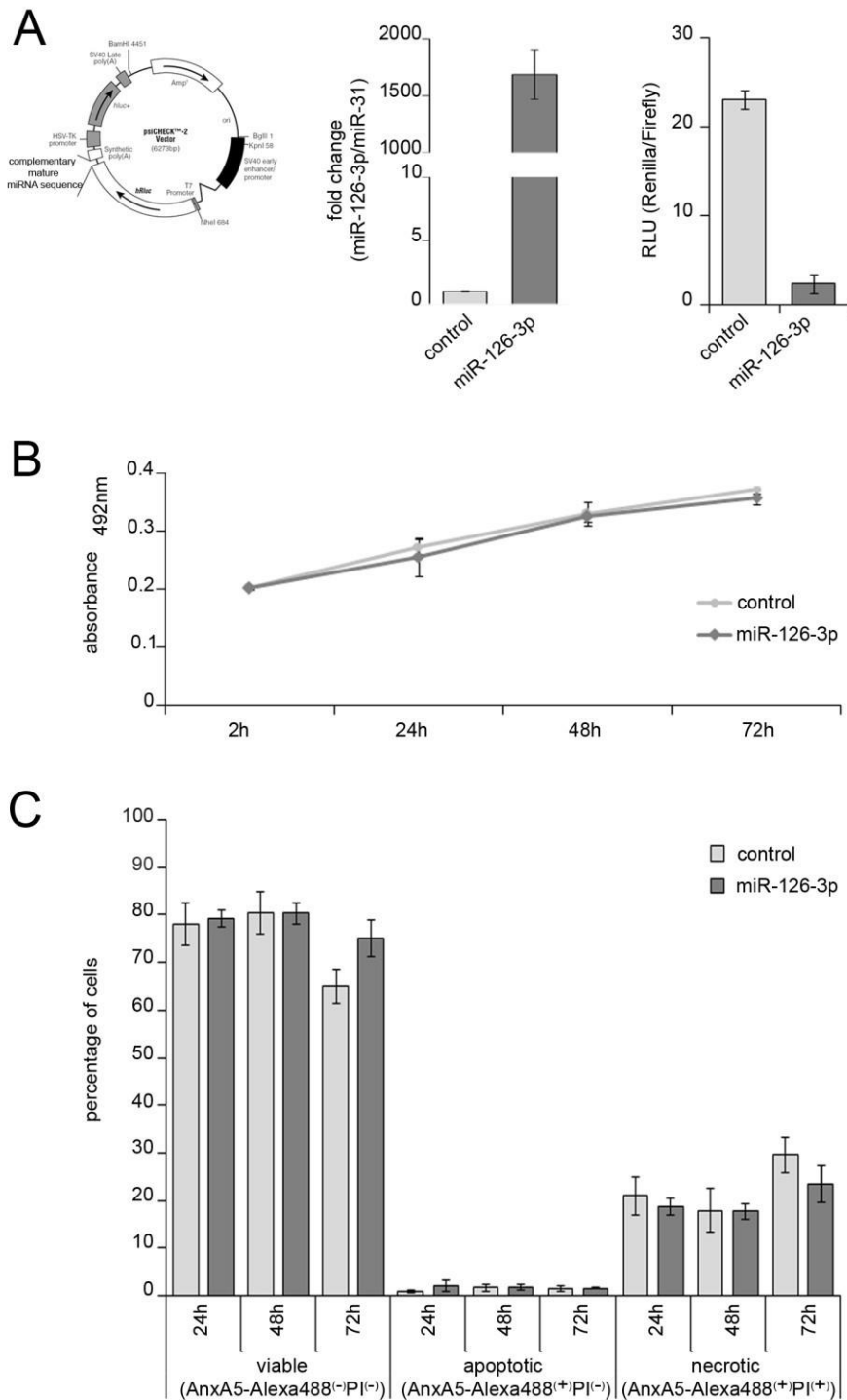
14
15
16

Supplemental figure 5

Characterization of aggregate and protrusion formation on collagen I gel and matrigel-coated surfaces

17
18
19
20
21
22
23
24
25
26
27
28
29
30
31
32
33
34
35
36
37
38
39
40
41
42
43
44
45
46
47
48
49
50
51
52
53
54
55
56
57
58
59
60

Cell cluster and protrusion formation of miR-126-3p control- or mimic- transfected PVC on 16µl of collagen I gel or matrigel. Representative images are shown.

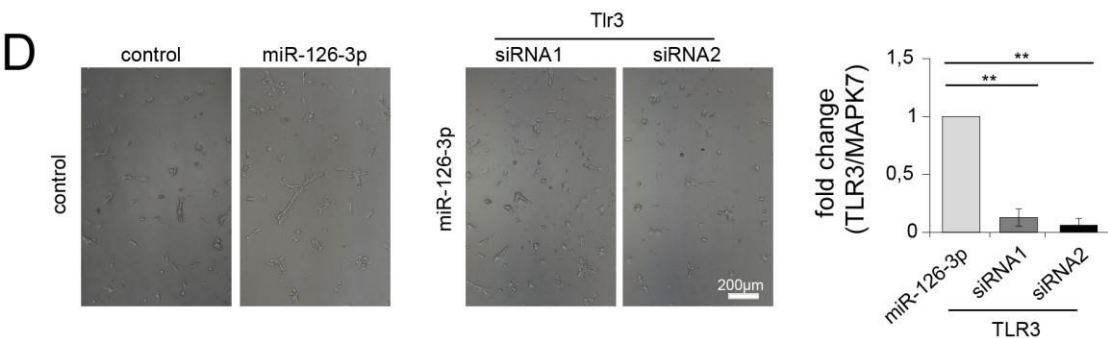
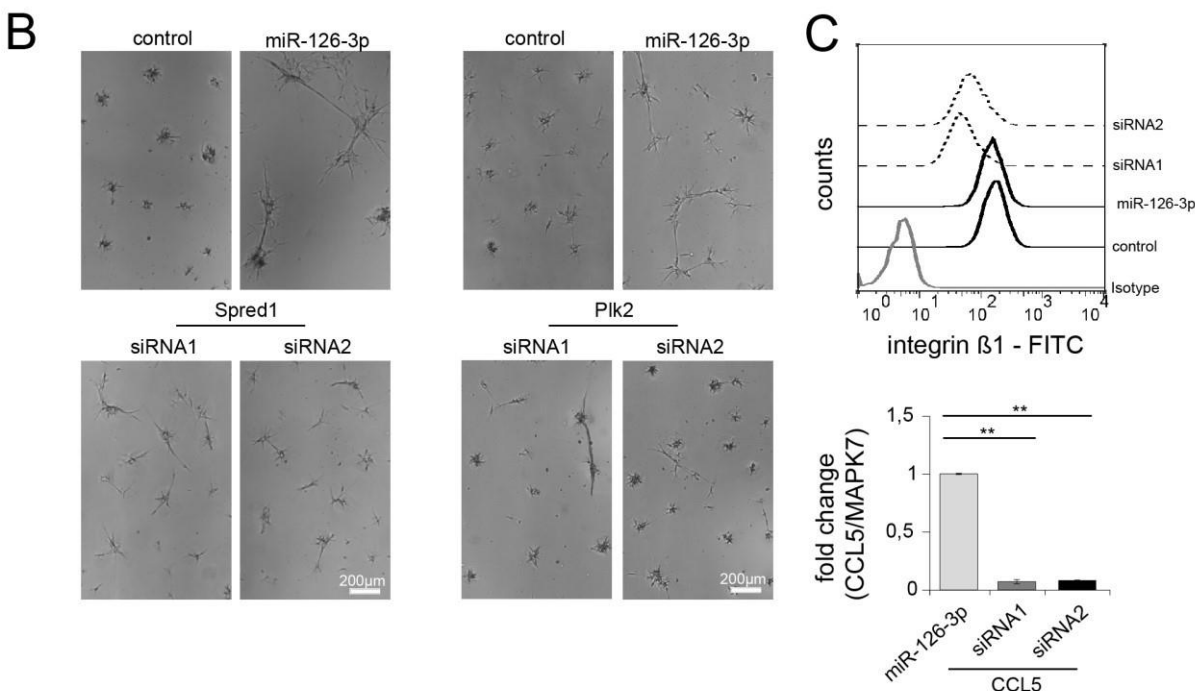
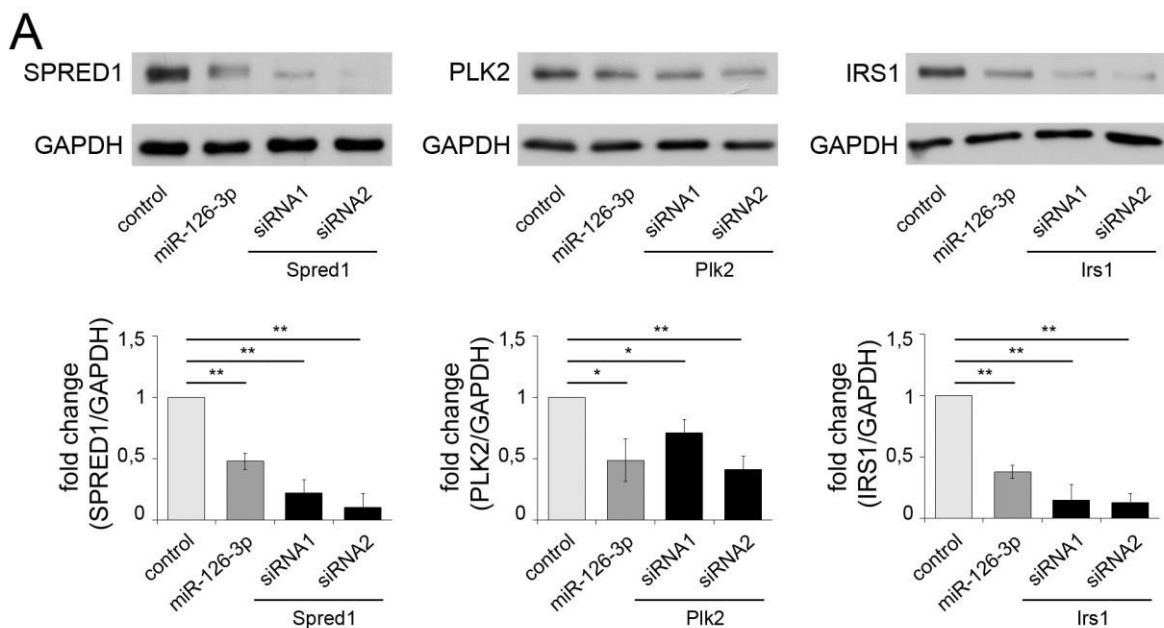


Supplemental Figure 6

Analysis of transfection efficiency, proliferation and viability in control- or miR-126-3p mimic-transfected PVC as well as characterization of network formation on growth factor-depleted matrigel

(A) Transfection efficiency and interaction of miR-126-3p with its target sequences was confirmed by luciferase reporter assays. The vector map depicts the coding sequence of Renilla luciferase (hRLuc), the multiple cloning site and the Firefly luciferase (hluc) normalizer (left). qPCR analysis of miR-126-3p expression in control- and mimic-transfected cells (center). The ratio of Renilla to Firefly luciferase activity in control- and miR-126-3p mimic-transfected cells was determined (right). (B) Cell proliferation was determined as the

1
2
3 production of a colored formazan product in metabolically active cells two, 24, 48 and 72
4 hours after transfection. (C) Cell viability was characterized by flow cytometry. The proportion
5 of AnxA5-Alexa488⁻/PI⁻ viable, AnxA5-Alexa488⁺/PI⁻ apoptotic and AnxA5-Alexa488⁺/PI⁺
6 necrotic cells 24, 48 and 72 hours post transfection was determined. (D) Cell cluster and
7 protrusion formation of miR-126-3p control- or mimic- transfected PVC on growth factor
8 reduced matrigel. Representative images are shown. The results of three independent
9 experiments were analyzed.
10
11
12
13
14
15
16
17
18
19
20
21
22
23
24
25
26
27
28
29
30
31
32
33
34
35
36
37
38
39
40
41
42
43
44
45
46
47
48
49
50
51
52
53
54
55
56
57
58
59
60



Supplemental Figure 7**Analysis of transfection efficiency in control-, miR-126-3p mimic- or siRNA-transfected PVC as well as characterization of network formation on matrigel**

Extracts of control-, miRNA-126-3p mimic-, siSpred1-, siPlk2- and silrs1-transfected PVC analyzed by immunoblotting. Two siRNA were transfected for each target gene. Fold change compared to control is given (graph). GAPDH was used for normalization. (B) Cell cluster and protrusion formation of control-, miR-126-3p mimic- or siRNA-transfected PVC on matrigel-coated surface 14 hours post plating. Representative images are shown. (C) Flow cytometry or qPCR analysis of β 1- integrin or Ccl5 knock down in transfected PVC. (D, left) Cell cluster and protrusion formation of control-, miR-126-3p-mimic or siTlr3-transfected PVC on matrigel coated surfaces 14 hours post plating. Representative images are shown. (D, right) qPCR analysis of siRNA-mediated knock down in miR-126-3p mimic- transfected cells. Three independent experiments were analyzed.

lrs1 fwd	tcgagCGTCTTCCTCTTCAGTAGATGGTACGATGCATgc
lrs1 rev	ggccgcATGCATCGTACCATCTACTGAAGAGGAAGACGc
lrs1 mut fwd	tcgagCGTCTTCCTCTTCAGTAGATGATTTCGATGCATgc
lrs1 mut rev	ggccgcATGCATCGAATCATCTACTGAAGAGGAAGACGc
miR-126-3p rep fwd	cgcCGATTATTACTCACGGTACGAgc
miR-126-3p rep rev	ggccgcTCGTACCGTGAGTAATAATGCGgcat
PIK3R2 hsa fwd	tcgagCTGGGAGGCAGGTTTTGTACGGTACGTTGTTAgc
PIK3R2 hsa rev	ggccgcTAACAACGTACCGTACAAAACCTGCCTCCCAGc
Pik3r2 mmu fwd	tcgagGATGGGAGCAGGTTTTGTACGGTACATTATTgc
Pik3r2 mmu rev	ggccgcAATAAATGTACCGTACAAAACCTGCTCCCATCc
Pik3r2 mmu mut fwd	tcgagGATGGGAGCAGGTTTTGTACGATTCATTTATTgc
Pik3r2 mmu mut rev	ggccgcAATAAATGAATCGTACAAAACCTGCTCCCATCc
Plk2 fwd	tcgagAGAGAAGTCGGACAGGTGGTGGTACGAATACAgc
Plk2 rev	ggccgcTGTATTCGTACCACCACCTGTCCGACTTCTCTc
Plk2 mut fwd	tcgagAGAGAAGTCGGACAGGTGGTGATTCGAATACAgc
Plk2 mut rev	ggccgcTGTATTCGAATCACCACCTGTCCGACTTCTCTc
Rgs3 fwd	tcgagCATCAGGTCCTTAACGCCCTGGTACGAGGGGAgc
Rgs3 rev	ggccgcTCCCCTCGTACCAGGGCGTTAAGGACCTGATGc
Rgs3 mut fwd	tcgagCATCAGGTCCTTAACGCCCTGATTCGAGGGGAgc
Rgs3 mut rev	ggccgcTCCCCTCGAATCAGGGCGTTAAGGACCTGATGc
Spred1 fwd	tcgagTTATATTTAACTAAATGTAAGGTACGAACTATgc
Spred1 rev	ggccgcATAGTTCGTACCTTACATTTAGTTAAATATAAc
Spred1 mut fwd	tcgagTTATATTTAACTAAATGTAAGATTCGAACTATgc
Spred1 mut rev	ggccgcATAGTTCGAATCTTACATTTAGTTAAATATAAc

Supplemental Table 1

Oligonucleotides used for the generation of the luciferase reporter constructs

Oligonucleotides containing the putative or mutated (mut, yellow nucleotides) miR-126-3p binding site are listed. mmu - Mus musculus, has – Homo sapiens